Report: DOE/ER/40723-1

BETA AND GAMMA DECAY HEAT MEASUREMENTS BETWEEN 0.1s - 50,000s FOR NEUTRON FISSION OF ^{235}U, ^{238}U AND ^{239}Pu

Progress Report

For Period June 1, 1992 To February 28, 1993

Walter A. Schier

DOE/ER/40723--1

DE93 012323

and

Gus P. Couchell

University of Massachusetts Lowell

Radiation Laboratory

Lowell, Massachusetts 01854

Prepared for

THE U.S. DEPARTMENT OF ENERGY

AGREEMENT NO. DE-FG02-92ER40723

ABSTRACT

A helium-jet/tape-transport system is employed in the study of beta-particle and gamma-ray energy spectra of aggregate fission products as a function of time after fission. During the initial nine months of this project we have investigated the following areas:

- Design, assembly and characterization of a beta-particle spectrometer
- Measurement of $^{235}U(n_{th},ff)$ beta spectra for delay times 0.2 s to 12,000 s
- Assembly and characterization of a 5"x5" NaI(Tl) gamma-ray spectrometer
- Measurement of $^{235}U(n_{th},ff)$ gamma-ray spectra for delay times 0.2s to 15,500s
- Assembly and characterization of HPGe gamma-ray spectrometer with a NaI(Tl) Compton-and-background-suppression annulus
- Measurement of $^{235}U(n_{th},ff)$ high-resolution gamma-ray spectra for delay times 0.6 s to over 100,000 s
- Comparison of individual gamma-line intensities with ENDF/B-VI
- Adaptation to our computer of unfolding program FERDO for beta and gamma aggregate fission-product energy spectra and development of a spectrum-stripping program for analysis of HPGe gamma-ray spectra
- Study of the helium-jet fission-fragment elemental transfer efficiency

This work has resulted in the publication of twelve BAPS abstracts of presentations at scientific meetings. There are currently four Ph.D. and two M.S. candidates working on dissertations associated with the project.

TABLE OF CONTENTS

A. INTRODUCTION

Although our knowledge of decay heat as a function of time after fission has shown steady improvement over the last two decades, few aggregate (integral) measurements have been conducted for delay times less than 10 s. Such measurements prove to be difficult due to the requirements of rapid fission foil transfer, short irradiation and counting times and the consequent high count rates necessary for adequate statistics. It also happens that decay heat predictions based on summation calculations of individual fission-product nuclei display their largest uncertainties for short delay times because of the incompleteness of the data base for the beta and gamma energy spectra of short-lived fission products and the resultant reliance on theoretical calculations to supplement the data base for this time region[1]. On the other hand it is estimated that almost 30% of the energy released by decay products in a reactor that has operated for a long time is obtained in the first 10 s after shutdown[2], clearly displaying the importance of short-lived products.

The present study will provide premium beta and gamma decay heat measurements for delay times as short as 0.1 s after fission and will extend to delay times up to 50,000 s. These measurements employ a helium-jet/tape transport system (Fig. 1) developed by us over the last several years for the study of delayed neutron (DN) spectra from fission products. This method has proved highly successful in measuring DN spectra as a function of delay time over successive time intervals between 0.17s and 85.5s[3-5]. Now separate aggregate beta and gamma-ray spectra measurements are made of the beta chains (Fig. 2) associated with the fission fragments.

Fission fragments are very rapidly transported from the neutron irradiated fission foil lining the fission chamber to the low background counting room by use of the helium jet. A very small fission chamber results in rapid flushing to maintain these short delay times (see Fig. 3). The fission fragments imbedded in microscopic oil droplets stick to the moving tape at the exit of the helium jet and are carried to the beta spectrometer or to beta detectors used in beta-gamma coincidence. By varying the tape speed or the detector position along the tape, the delay time can be varied.

Aspects of defining delay time and accumulating good statistics are now separated in the helium jet case. The measurement of a spectrum is made for a fixed delay-time interval by maintaining the tape speed constant and it proceeds until good statistical quality is achieved. Count rates can always be maintained at reasonable levels by adjusting the neutron flux at the fission chamber, thus count rates produce no appreciable adverse effects such as degraded energy resolution, substantial deadtime corrections, pulse pile-up effects, etc. Furthermore, because beta-gamma coincidences are used for gating the gamma-ray spectra, background effects are reduced by two orders of magnitude. This coincidence feature greatly enhances our

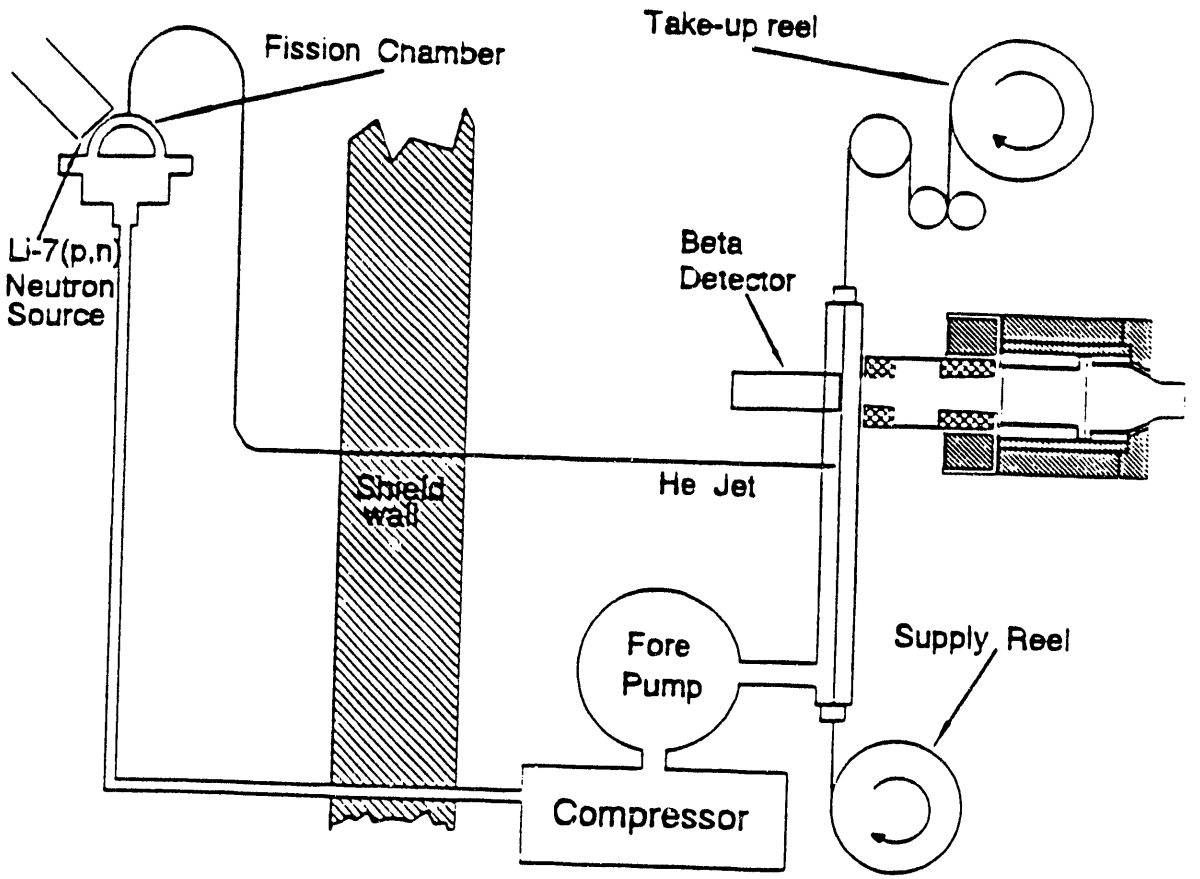

Fig. 1. Diagram of the helium-jet/tape-transport system with NaI spectrometer.

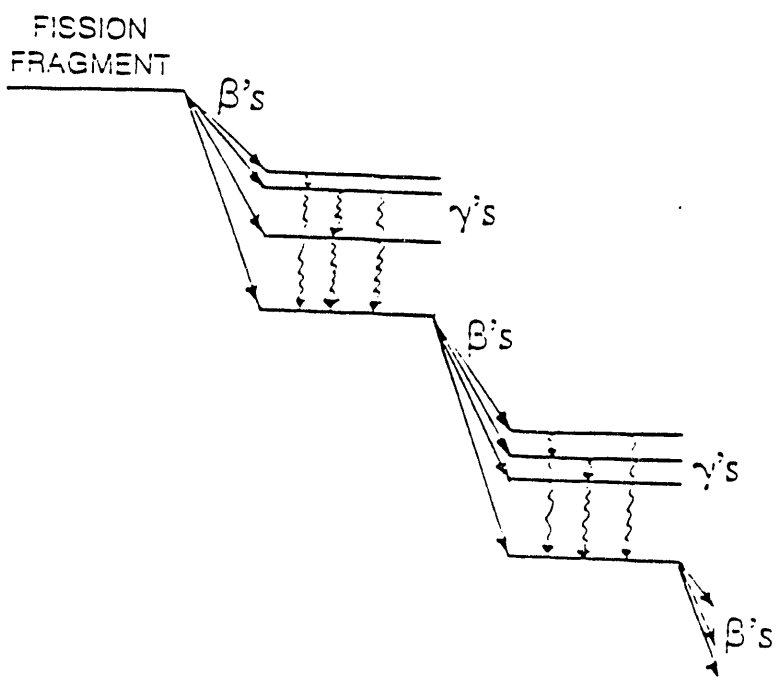

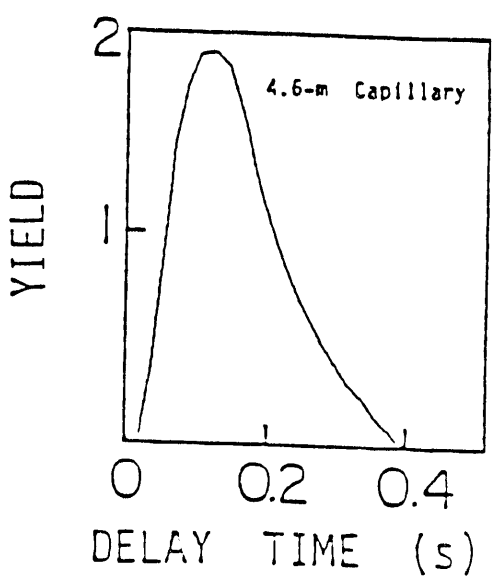

Fig. 2. Beta chain with accompanying gammas. *Fig. 3. Transfer time of He-jet.*

sensitivity to high energy gamma rays, and also suppresses our sensitivity to beta-ray bremsstrahlung which is primarily forward-peaked and thus heads away from the gamma-ray detector.

In addition, by the use of a germanium detector in conjunction with a NaI annulus for Compton suppression, this method is particularly well suited to the measurement of discrete gamma lines associated mainly with single individual isotopes in the beta chains. These high resolution spectra should prove valuable in providing several hundred tests of the gamma activity from fission products comprising the data bases. In particular, such studies should shed light on isomeric states which are cited[6] as causing substantial changes in decay heat values.

In order to facilitate the comparisons between our measurements and summation calculations, we have established a collaboration with Dr. Talmadge England at the Los Alamos National Laboratory. As part of this collaboration, one of our graduate students (Joann Campbell) has spent three months the last two summers at LANL, supported in part by the UMass Lowell and in part by LANL. Under the supervision of Dr. England, she has become familiar with the computational facilities and has assisted him in making detailed comparisons between summation calculation predictions of the beta and gamma-ray decay heat spectra and our experimental results.

In the meantime our experimental program has made significant progress during the first nine months of this funding period. We have built or assembled all the components of out beta spectrometer, NaI detector with its shield and high-resolution HPGe detector with its NaI annulus for Compton and background suppression. Response functions at a number of incident energies have been measured for both the beta and NaI spectrometers. Unfolding of the continuous beta- and gamma-ray spectra resulting from our decay heat measurements will be performed using the program FERDO[7], recently obtained from the Radiation Shielding Information Center of ORNL, and currently being adapted for our computational facilities. Another computer program (NDAA) has been written and applied in obtaining peak areas in high-resolution gamma-ray spectra obtained with our HPGe system. Each of these spectrometers has been used to study decay heat activity following thermal neutron fission of ^{235}U. Premium beta spectra have been measured at selected time intervals ranging from 0.2 to 12,000 s. NaI gamma-ray spectra have been obtained for delay times 0.2 to 15,440 s and HPGe spectra were measured over a delay time range 0.6 to over 100,000 s. The use of beta-gamma coincidence in the gamma-ray measurements has produced spectra of excellent statistical quality and extremely low background, attainable currently only with a helium-jet transfer system. Once the continuous beta and gamma spectra are unfolded using the FERDO program, these measurements will be compared with summation calculations with the assistance of Dr. England. Spectra measured at delay times at least an-order-of-magnitude shorter

than have been previously reported will provide interesting checks of the "Gross Theory" of beta decay[8-10] for short-lived fission products far from the line of stability. In addition hundreds of gamma-ray lines have been stripped from our HPGe spectra, allowing detailed comparisons of individual fission-product activity with the ENDF/B-VI data base used in decay heat summation calculations.

B. BETA SPECTROMETER

A beta spectrometer was designed, tested and refined to measure beta spectra and extract the average beta energy as a function of time after fission for delay times ranging from 0.1 to 50,000 s. A cross sectional view of the spectrometer is given in Fig. 4. The beta detector is essentially a large plastic scintillator (6.4 cm diameter x 8.9 cm long, BC 408, Bicron Corp.) with a well (3.8 cm diameter x 2.5 cm deep) in its front face where the betas are incident. This well-scintillator provides 100% intrinsic detection efficiency, a substantial solid angle, good linearity, adequate energy resolution (e.g. 12% FWHM at 1 MeV) for the full beta energy range of 0 to 10 MeV and a relatively simple response function to monoenergetic electrons.

But perhaps the spectrometer's most crucial feature is the excellent gamma ray rejection. This is such an important aspect because in the beta decay chains the number of gamma rays emitted exceeds the number of betas. This gamma ray rejection is accomplished by optically isolating the well-scintillator with a thin aluminum foil and placing a very thin scintillator disk (0.05 cm thick x 3.8 cm diameter) at the mouth of the well. This thin disk is viewed by two photomultipliers. Incident betas passing through the disk provide a coincidence pulse which signals an incident beta particle. Gamma rays seldom interact with the disk and are, therefore, very effectively discriminated. This gamma rejection is demonstrated in Fig. 5a with a bare ^{24}Na beta (and gamma) source while at the same time an intense, 50 μCi, encapsulated ^{22}Na gamma source is placed near the ^{24}Na beta source. The pulse height with the disk coincidence turned off displays a spectrum dominated by the Compton bands of the ^{22}Na 0.511- and 1.274-MeV gamma rays. With the coincidence gate active, the gamma pulses are very effectively rejected (Fig. 5b) leaving essentially only the ^{24}Na beta spectrum. This spectrum has nearly the calculated shape for this allowed beta decay.

A second benefit of gating on the disk pulse is that edge effects are nearly eliminated from measured beta spectra. This is because the diameter of the disk is considerably smaller than the 8.9 cm daimeter of the well-scintillator. Only betas that enter the well are measured. The secondary electrons produced in the detection process cannot readily escape the boundaries of the scintillator. Measured beta source spectra, therefore, rather faithfully reproduce the calculated beta energy spectrum shape.

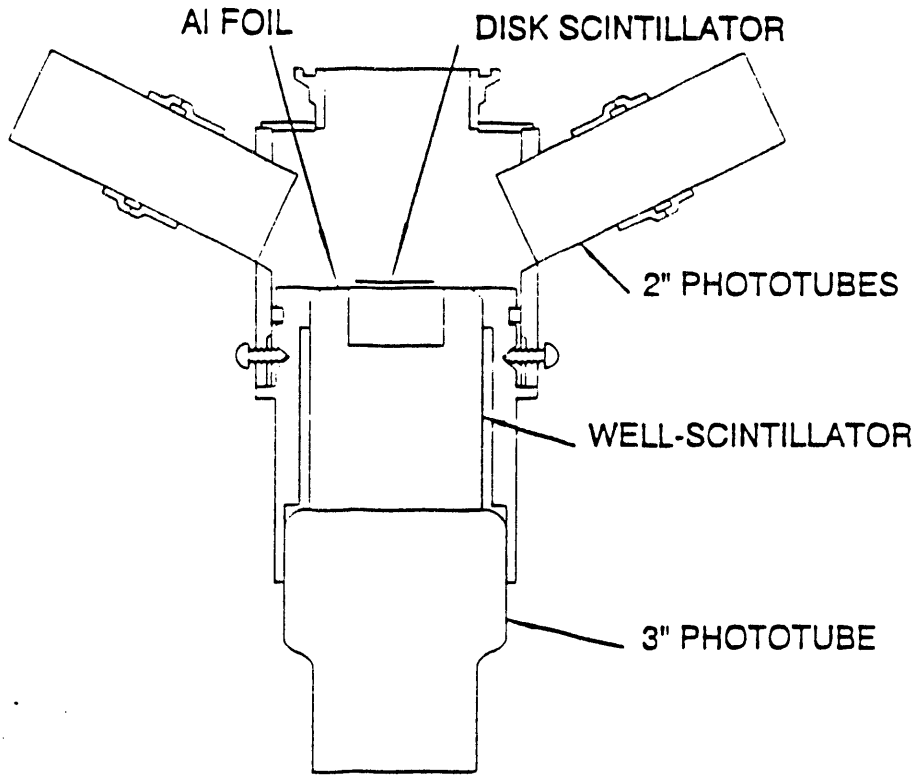

Fig. 4. Cross sectional view of the beta spectrometer.

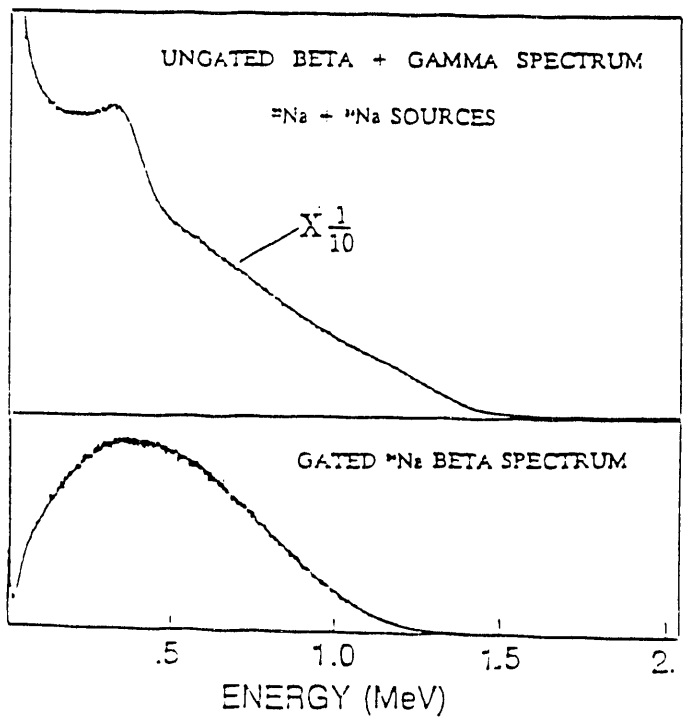

Fig. 5. Spectra showing rejection of severe gamma-ray background with disk gating.

The measurement of response functions for monoenergetic electrons is preferred over computer simulations because measurements take into account not only lost secondary electrons from the scintillator but also beta scattering interactions with the spectrometer housing. Bare sources with energetic internal conversion electrons are desireable because they emit in a 4π manner and thus these response functions would include the scattering events external to the scintillator. Presently we are using three bare IT sources, Sn/In-113m, Cs-137 and Bi-207 for monoenergetic electrons in the 0 to 1-MeV range. Each IT source has its own complications in the measurement of response functions. Take, for example, the well-known Cs-137 source which beta decays to the 662-keV isomeric state in Ba-137 having a 2.6 minute halflife. To reject the beta continuum which would obscure the response function "low energy" tail, a coincidence with barium K-shell x rays is performed. Due to the state's long lifetime, this coincidence discriminates away the beta continuum as demonstrated in Fig. 6. For Bi-207, two major internal conversion electron lines at energies of 481- and 976-keV would be superimposed in the spectrum. To extract each response function separately, a coincidence with the 0.570-MeV gamma ray produces a measured 976-keV electron response function and with the 1.770-MeV gamma ray, a measured 481-keV electron response function. Such beta spectrometer response functions measurements form a part of the Ph.D. thesis of Shengjie Li.

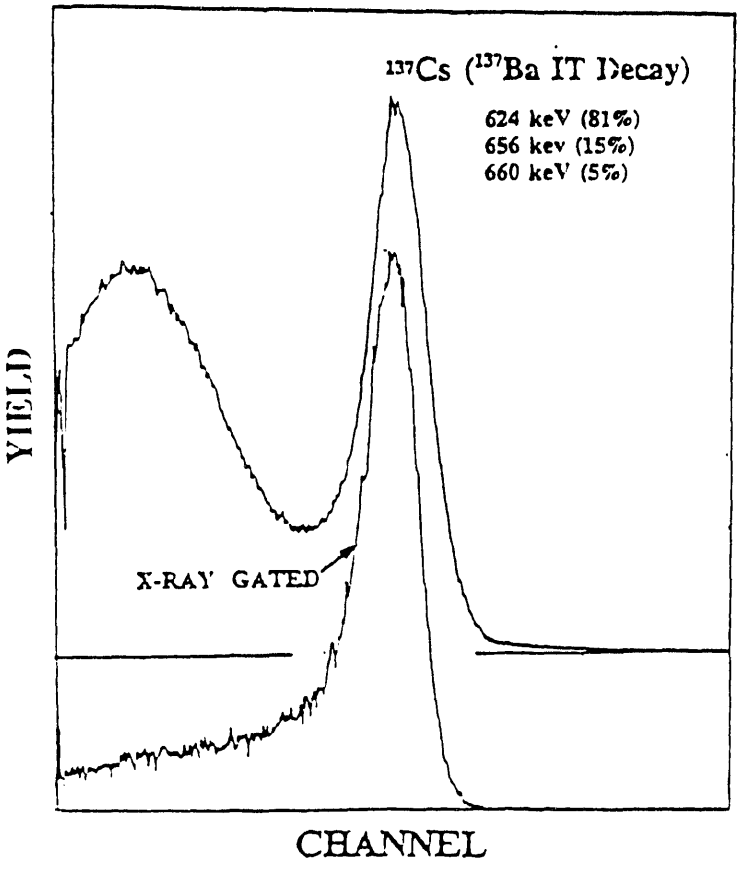

Fig. 6. Beta response function using a bare ^{137}Cs and x-ray coincidence.

C. $^{235}U(n_{th}, ff)$ BETA SPECTRA FOR DELAY TIMES 0.2 s TO 12000 s

Aggregate beta spectra following the thermal neutron fission of ^{235}U have been measured at seventeen time intervals spanning the delay time range 0.2 to 11,960 s. These are the first beta spectra measurements below a delay time of 2 s and the only corroborating measurement below 20 s with previous measurements[11]. These spectra have been nested in Figs.7 and 8 to demonstrate the statistical quality of the spectra and the decrease in the beta spectrum's average energy as delay time increases. On the linear scale (Fig.7) the "peak" width decreases with energy and on the log scale (Fig.8) one observes the end point energy shifting to lower values at longer delay times. Spectra at short times also display electron lines from internal transitions superimposed on the aggregate continuous beta spectra. These spectra will be analyzed with the reponse function unfolding program (FERDO) to extract the "true" energy distributions and their average energies and compare them to ENDF/B-VI. These ^{235}U beta spectra measurements and their analysis form a portion of the Ph.D. thesis of Shengjie Li.

D. NaI SPECTROMETER

The gamma-ray component of decay heat is measured using a 5" x 5" NaI(Tl) detector. The detector is housed in a massive shield consisting of a combination of lead, brass and tungsten as depicted in Fig.9. Tungsten is used in the front snout which defines the solid angle of the detector. Whereas the diameter of the NaI scintillator is 5", the diameter of the tungsten aperture adjacent the scintillator is 3" in order to minimize edge effects. The magnet in the nose of the shield deflects beta particles away from the detector, so that it sees only the gamma component of the tape activity. The tape bearing the fission products travels perpendicular to the plane of the figure. A thin beta detector is located on the opposite side of the transport tape as shown. Beta-gamma coincidences are used to gate the NaI spectrum. Although the NaI detector is well shielded and views only a limited portion of the tape, the beta detector which is tightly collimated truely defines the region of the tape viewed, and thus delay time following fission. Equally important, beta-gamma coincidence reduces background, including that due to betas that pass through the magnetic deflection system, by approximately two orders of magnitude.

Gamma-ray decay heat spectra measured with the NaI detector consist of hundreds of lines and thus display a rather smooth variation with energy, i.e., there are no clearly resolvable peaks. In order to obtain the "true" energy distribution of the emitted gammas, these spectra must be corrected for the detector response function. Since the response function varies with incident gamma-ray energy, it must be measured using monoenergetic gamma rays from various sources. Table I lists possible one- and two-prominent-photopeak sources which span the energy range of

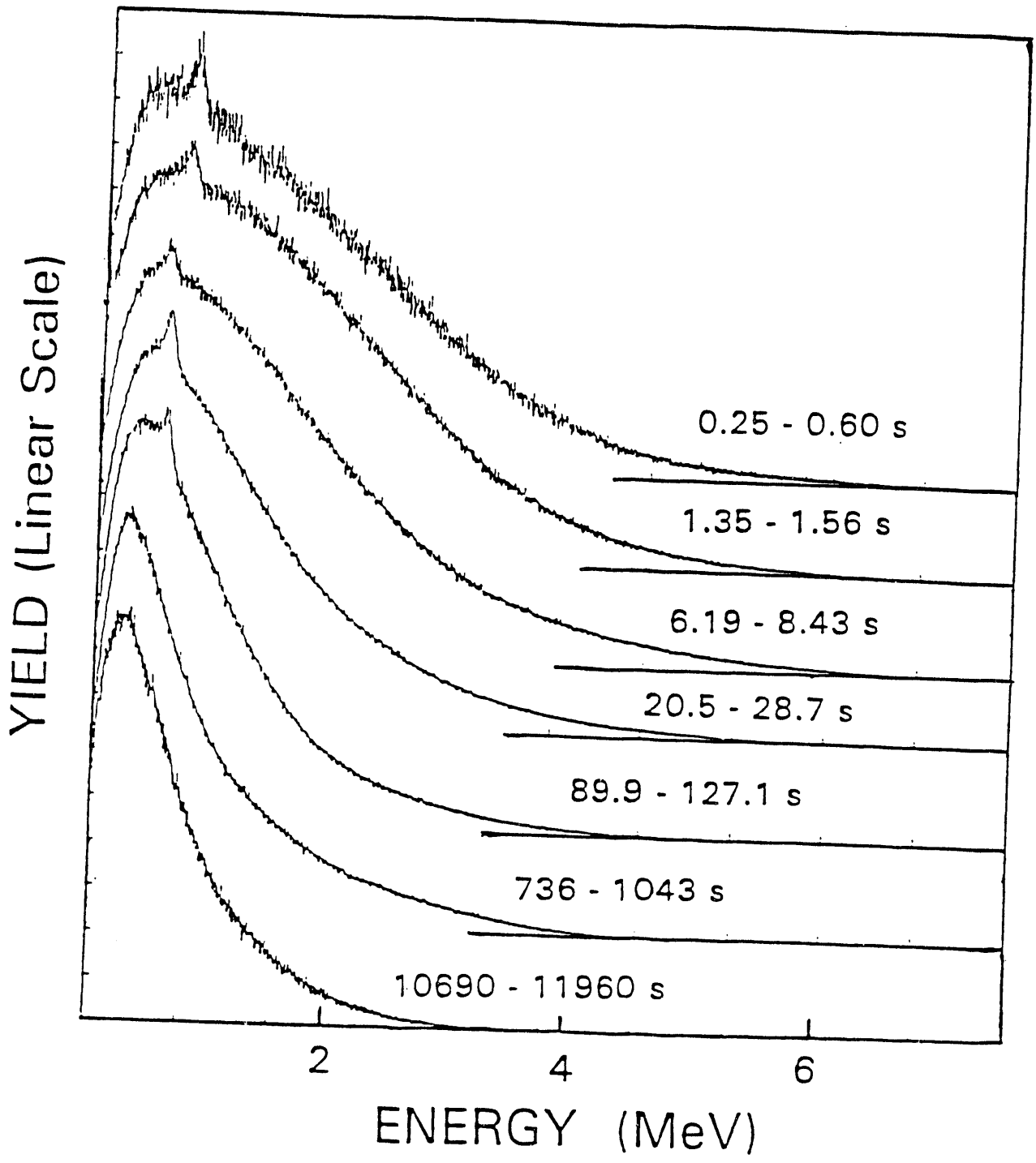

Fig. 7. $^{235}U(n_{th}, ff)$ beta spectra measurements at some representative time intervals.

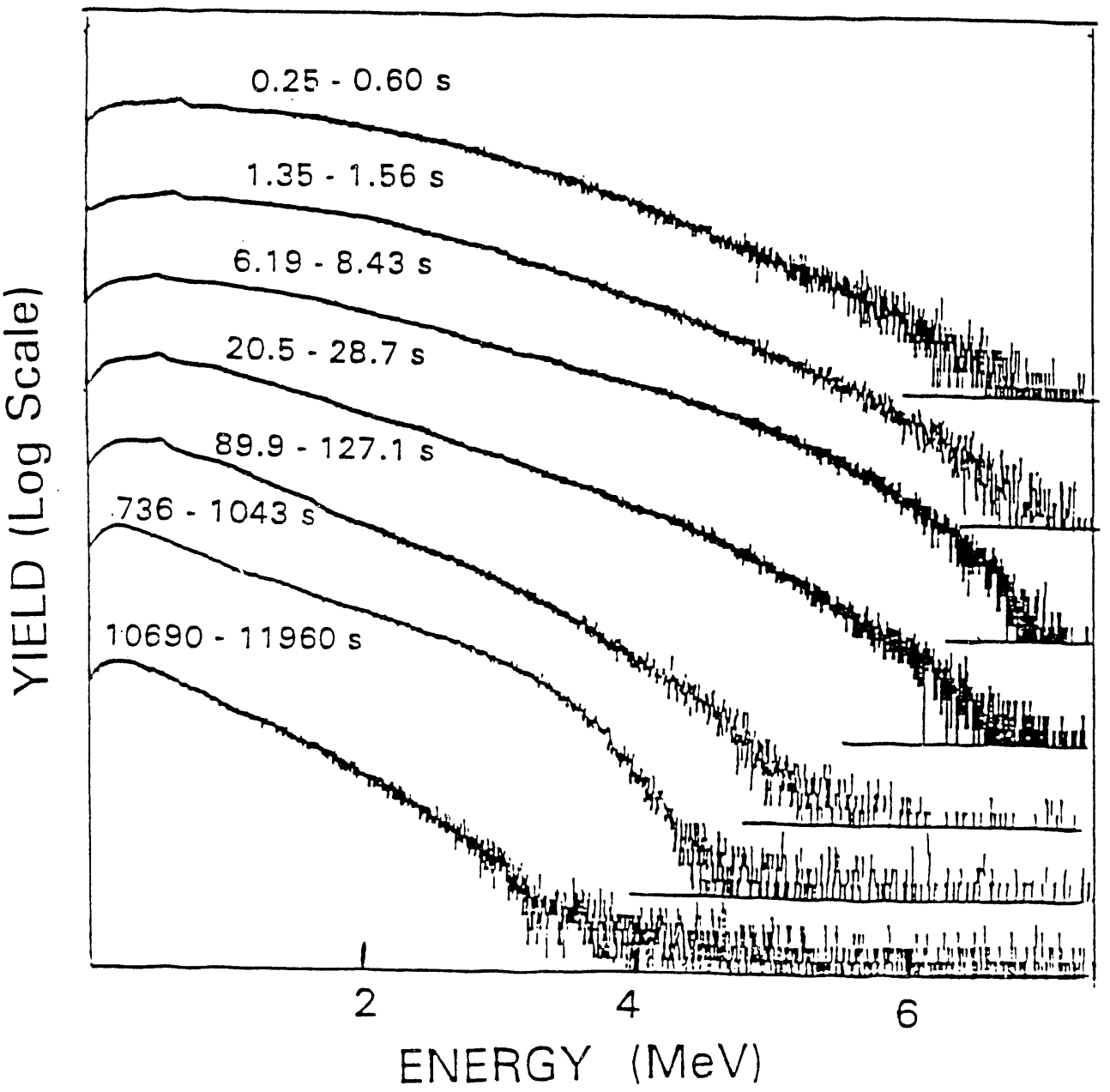

Fig. 9. Beta spectra in Fig. 8 replotted on log scale to reveal the end point energies.

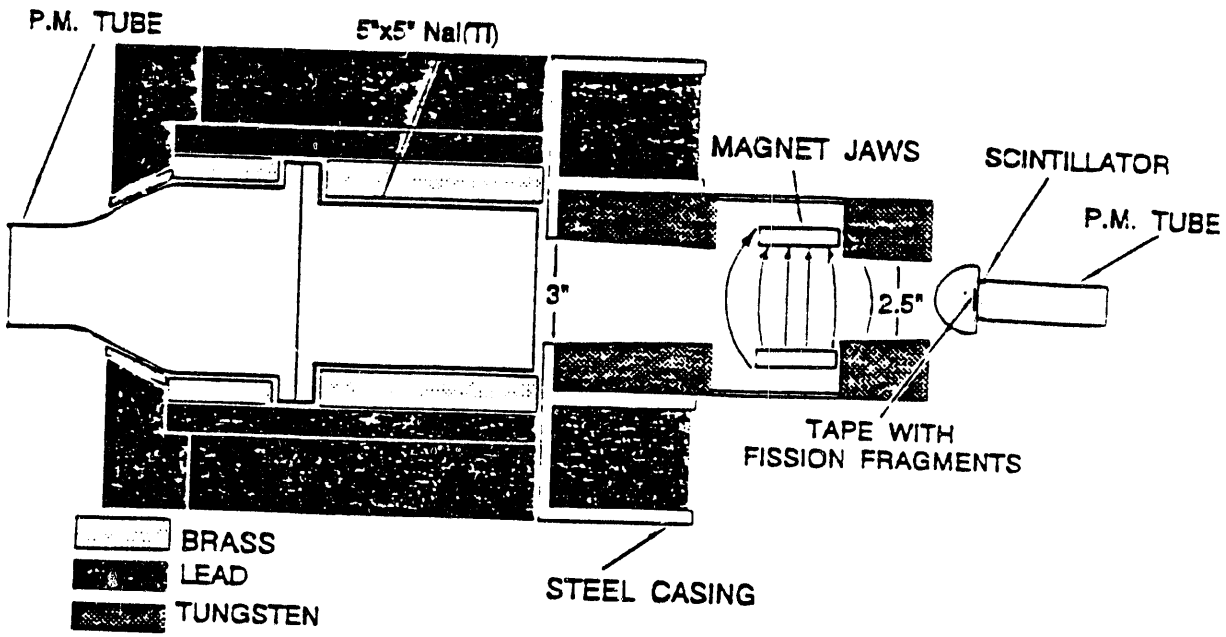

Fig. 9. NaI(Tl) spectrometer with collimator and shield. Beta detector is also shown.

Table I. Gamma-ray sources for determining NaI response functions.

E_γ (MeV)	Isotope	$T_{1/2}$	Decay mode
0.060	^{241}Am	433 y	α
0.088	^{109}Cd	1.30 y	EC
0.121	^{57}Fe	2.62 y	β
0.166	^{139}Ce	138 d	EC
0.279	^{203}Hg	46.6 d	β
0.412	^{198}Au	2.7 d	β
0.662	^{137}Cs	30.1 y	β
0.835	^{54}Mn	313 d	EC
0.847	^{56}Mn	2.58 h	β
1.115	^{65}Zn	244 d	EC, β
1.173	^{60}Co	5.27 y	β
1.332	^{60}Co	5.27 y	β
1.369	^{24}Na	15.0 h	β
1.525	^{42}K	12.4 h	β
1.642	^{38}Cl	37.2 m	β
1.811	^{56}Mn	2.58 h	β
2.167	^{38}Cl	37.2 m	β
2.754	^{24}Na	15.0 h	β
4.434	^{12}C	----	$^{9}Be(\alpha,n)$
6.130	^{16}O	----	$^{19}F(p,\alpha)$

! Two transitions

interest in gamma-ray decay heat studies, 0 to 7 MeV. A sample of recently measured response functions is shown in Fig.10. These spectra illustrate the variation of detector response with gamma-ray energy. Many of the sources listed in Table I, e.g. ^{198}Au and ^{24}Na, can be produced through neutron activation using our 1-MW swimming-pool reactor. The ^{19}F(p,$\alpha\gamma$)^{16}O* reaction was used to produce the 6.13-MeV line from ^{16}O. This measurement was performed using our 2-MV Van de Graaff accelerator. The 0.511-MeV lines seen in the ^{24}Na and ^{16}O response functions are the result of pair production in the collimator and shield surrounding the detector. The determination of NaI response functions is ongoing, and these studies form part of Edward Seabury's Ph.D. thesis project.

E. ^{235}U(n_{th}, ff) GAMMA-RAY SPECTRA FOR DELAY TIMES 0.2 s TO 15500 s

Aggregate gamma-ray spectra following the thermal neutron fission of ^{235}U have been measured with our 5"x5" NaI spectrometer at 16 time intervals spanning the delay time range 0.2 to 15,440 s. These are the first gamma-ray spectra measurements below a delay time of 1 s. These spectra have been nested in Figs.11 and 12 to demonstrate the statistical quality of the spectra and the change in character as delay time increases. On the linear scale (Fig. 11) the new "peaks" arise as energy decreases and on the log scale (Fig.12) one observes the end point energy shifting to lower values at longer delay times. There is considerable interest in the nature of spectra at short delay times where the "Gross Theory" of beta decay predicts a higher yield in the high-energy region than is supported by experimental studies of the gamma-ray spectra from individual fission products. These spectra will be analyzed with the reponse function unfolding program (FERDO) to extract the "true" energy spectra and their average energies. These will be compared to ENDF/B-VI data base which is supplemented by the "Gross Theory" of beta decay for most fission products possessing high Q-values. These ^{235}U gamma-ray spectrum measurements and their analysis comprise a part of the Ph.D. thesis of Edward Seabury.

F. HPGe DETECTOR WITH NaI COMPTON SUPPRESSION ANNULUS

A high purity germanium detector with 1.8-keV resolution (^{60}Co), purchased from Canberra Inc., is used in high resolution measurements of fission product gamma-ray lines. A NaI(Tl) annulus is also used with the detector to suppress contributions from Compton gamma-rays in the spectra. The system geometry is shown in Fig.13. To maintain satisfactory count rates during measurements it is desirable to position the HPGe detector close to the fission product activity on the tape. To accomplish this the detector was designed with a longer cryostat pipe than is usual in order to bring the detector to the front face of the annulus rather than the

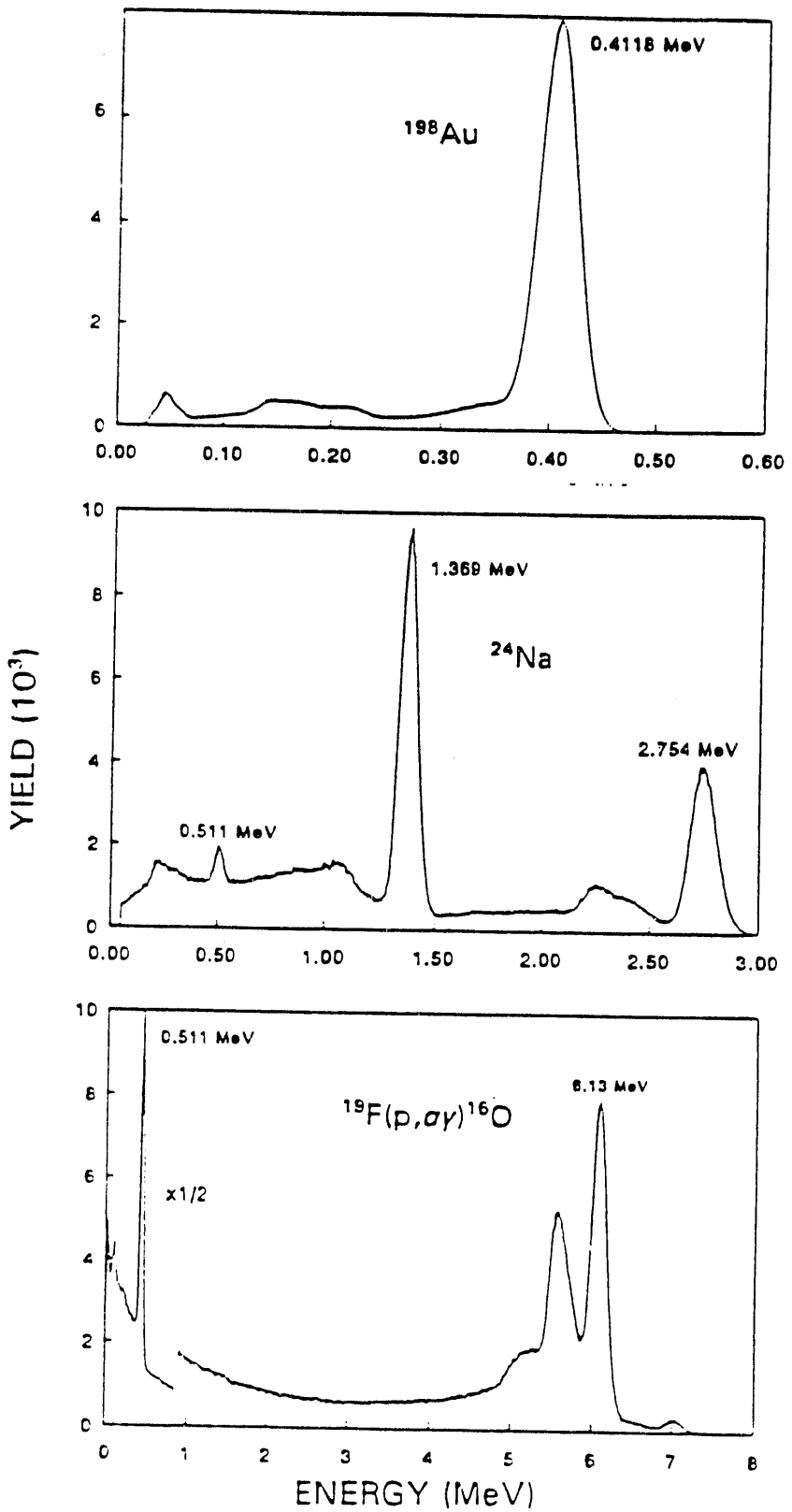

Fig. 10. NaI response functions measured at some representative energies.

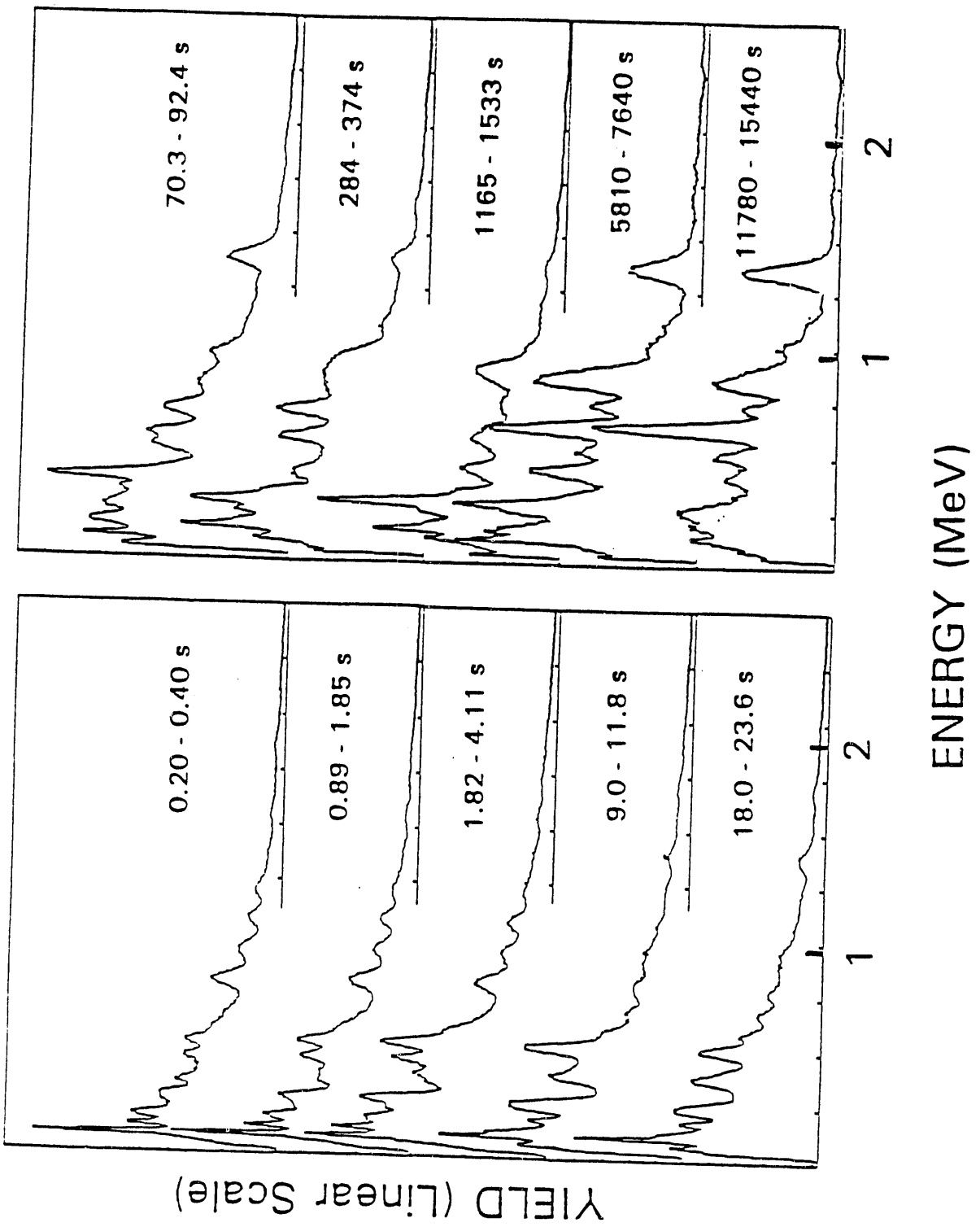

Fig. 11. *$^{235}U(n_{th},ff)$ gamma-ray spectra measurements with NaI at some representative delay times.*

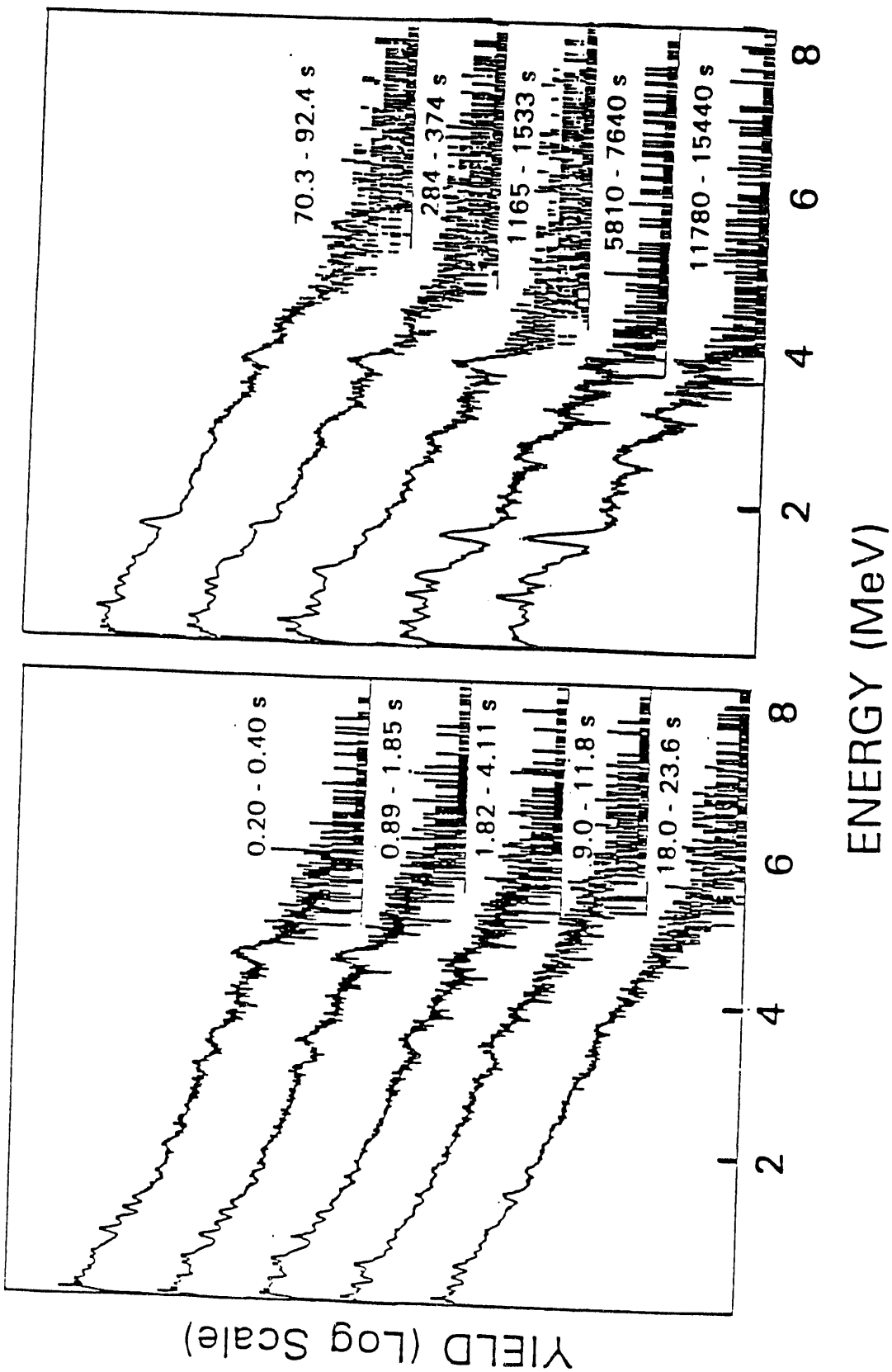

Fig. 12. Spectra in Fig. 11 replotted on log scale to view the high energy gammas.

center. Although this geometry results in reduced annulus efficiency, the peak-to-background ratio in the gamma-ray spectra is still greatly improved. This can be seen in the spectra of Fig.14, measured for $^{235}U(n_{th}, f)$ with and without Compton suppression. The delay interval following fission was 0.58 - 0.90 s and in both cases beta-gamma coincidence gating was employed. Two energy regions are shown: 0 - 1.5 MeV and 3.0 - 4.5 MeV. The peak-to-background ratio is improved by a factor 2.9 over the lower region and by 4.7 over the upper region. This improvement not only allows the measurements to extend to weaker gamma-ray peaks but also extends the time intervals over which the time evolution of individual peaks can be followed. This is important for identifying isotopes which contribute to the gamma spectra.

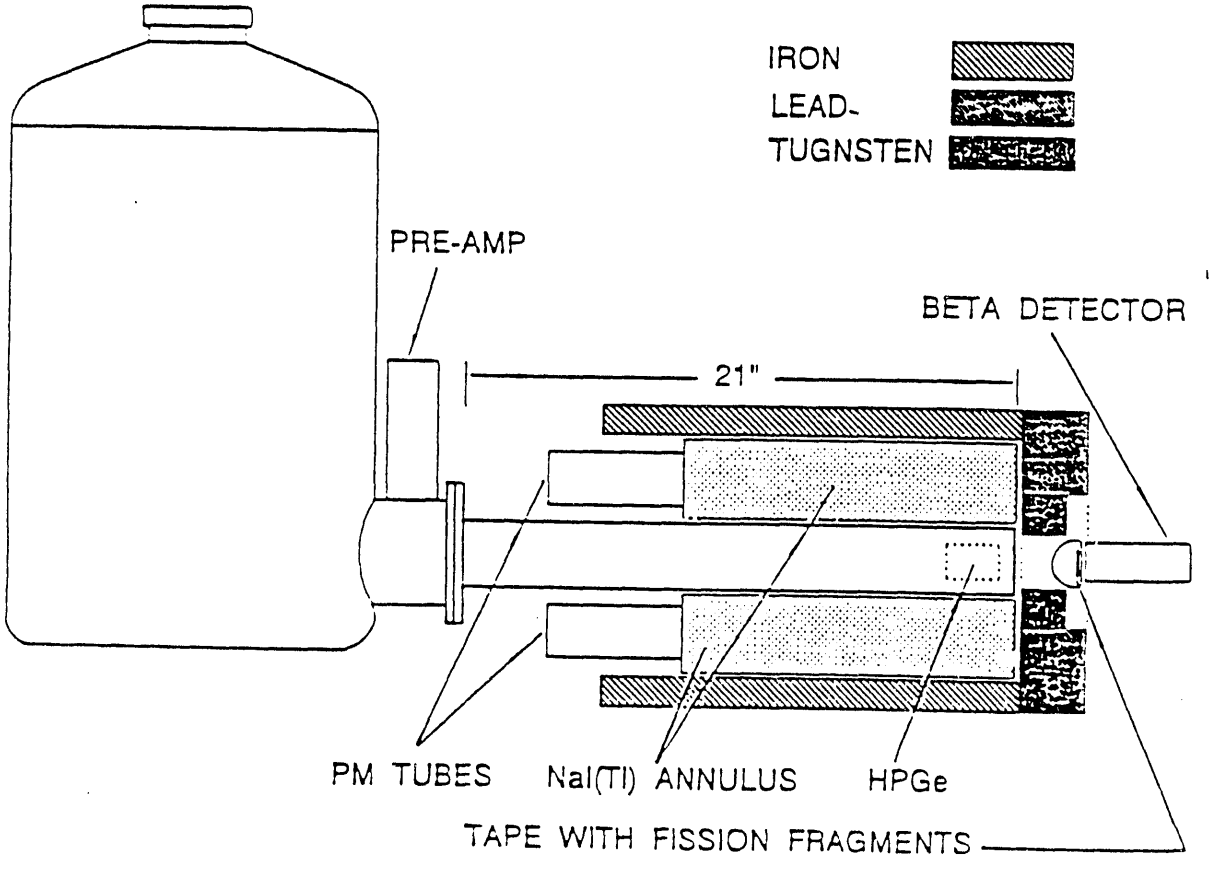

Fig. 13. HPGe spectrometer with Compton and background suppression annulus. The beta detector is also shown.

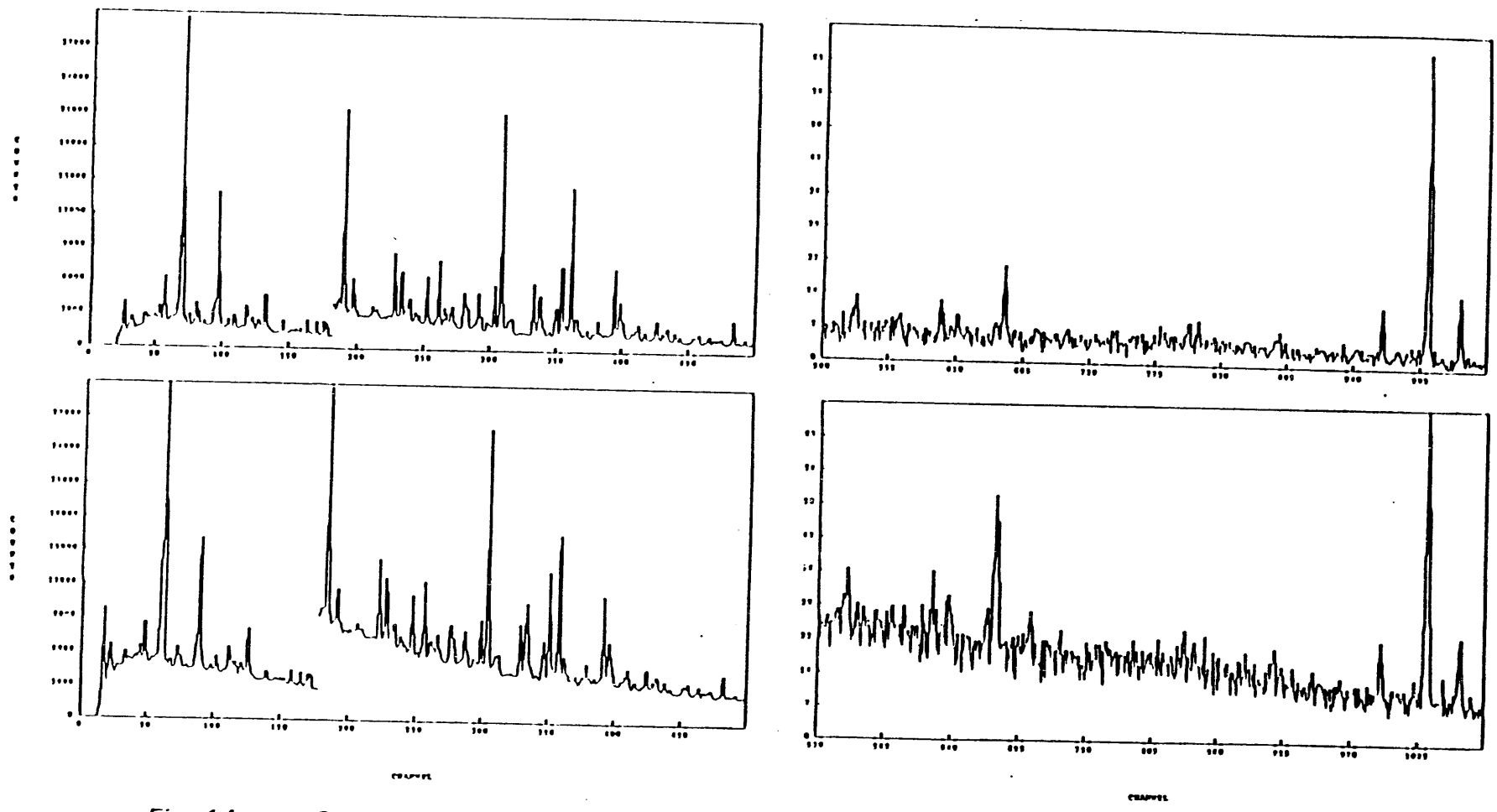

Fig. 14. *Gamma-ray spectra measured for $^{235}U(n_{th}, f)$ for the time interval 0.58 - 0.90s following fission. The two spectra to the left cover the gamma energy range 0 - 1.5 MeV and the two to the right correspond to the range 3 - 4.5 MeV. The two upper spectra were measured with the NaI(Tl) Compton suppression annulus and the two lower spectra were measured without suppression. Both spectra were measured with beta-gamma coincidence.*

G. $^{235}U(n_{th},ff)$ HIGH RESOLUTION GAMMA SPECTRA, 0.6 s TO OVER 100,000 s

Gamma-ray spectra have been measured with this detector for fifteen delay time intervals following fission, covering the range 0.6 to over 100,000s. Analysis of these spectra is currently in progress and an example spectrum, corresponding to the interval 0.58 - 0.90 s and covering the gamma energy range 0 to 6 MeV, is shown in Figs. 15 and 16. Gamma-ray peaks extracted from this spectrum are listed in Table II. Only those peaks whose area counts exceed the local background area by at least two standard deviations are included in the table, which amounts to 286 such peaks (including also single and double escape peaks). Almost half of these have energies less than 1 MeV and no peaks are observed above 4.6 MeV.

Several fission products have been identified and these are indicated in the spectrum. Although very rich in gamma lines, the spectra are nevertheless quite selective in the nuclides which are the predominant contributors. This selectivity results from the enhancement which occurs for those nuclides having beta-decay halflives which approximately match the delay interval following fission. Shorter-lived precursors will have largely died away whereas longer lived ones will not decay appreciably during the selected interval. For example, the principal nuclide contributors identified so far in Figs.15 and 16 have halflives of 0.40s (^{97}Sr), 0.65s (^{96}Y), 0.7s (^{98}Sr), 1.1s (^{96}Sr), 1.21s (^{98m}Y), and 2.1s (^{98}Zr) which are all comparable to the measurement times in the of 0.58 - 0.90 s interval.

H. BETA COUNT-RATE MEASUREMENTS

The beta activity resides on the moving tape of the helium-jet/tape transport system. For a constant tape velocity, a given distance along the tape downstream from the helium-jet spray point corresponds to a specific delay time. Our present 4.6-m helium-jet capillary[3] introduces an average delay of 0.16 s with a FWHM spread of 0.15 s. In future measurements, the capillary will be further shortened to about 3 m to achieve a mean delay time and a time spread of only 0.1 s each. The measurement of beta count rate as a function of delay time can be performed using two thin-scintillator detectors along the tape, one that is fixed (the monitor) and one that is moveable. Beta count rates are acquired for each detector in a multiscaling mode and a ratio of corresponding portions of the multiscaler outputs provide relative normalization. The 0.25-mm thick plastic scintillators are very insensitive to gamma rays and the scintillator geometry enters only in calculating the small delay-time interval spanned. Our system can also measure beta count rates in the more conventional manner. In this case the tape bearing the activity is stopped, the beta activity remains stationary at the beta detector and the time dependence of the activity is measured by multiscaling. We get good agreement between both measuring techniques.

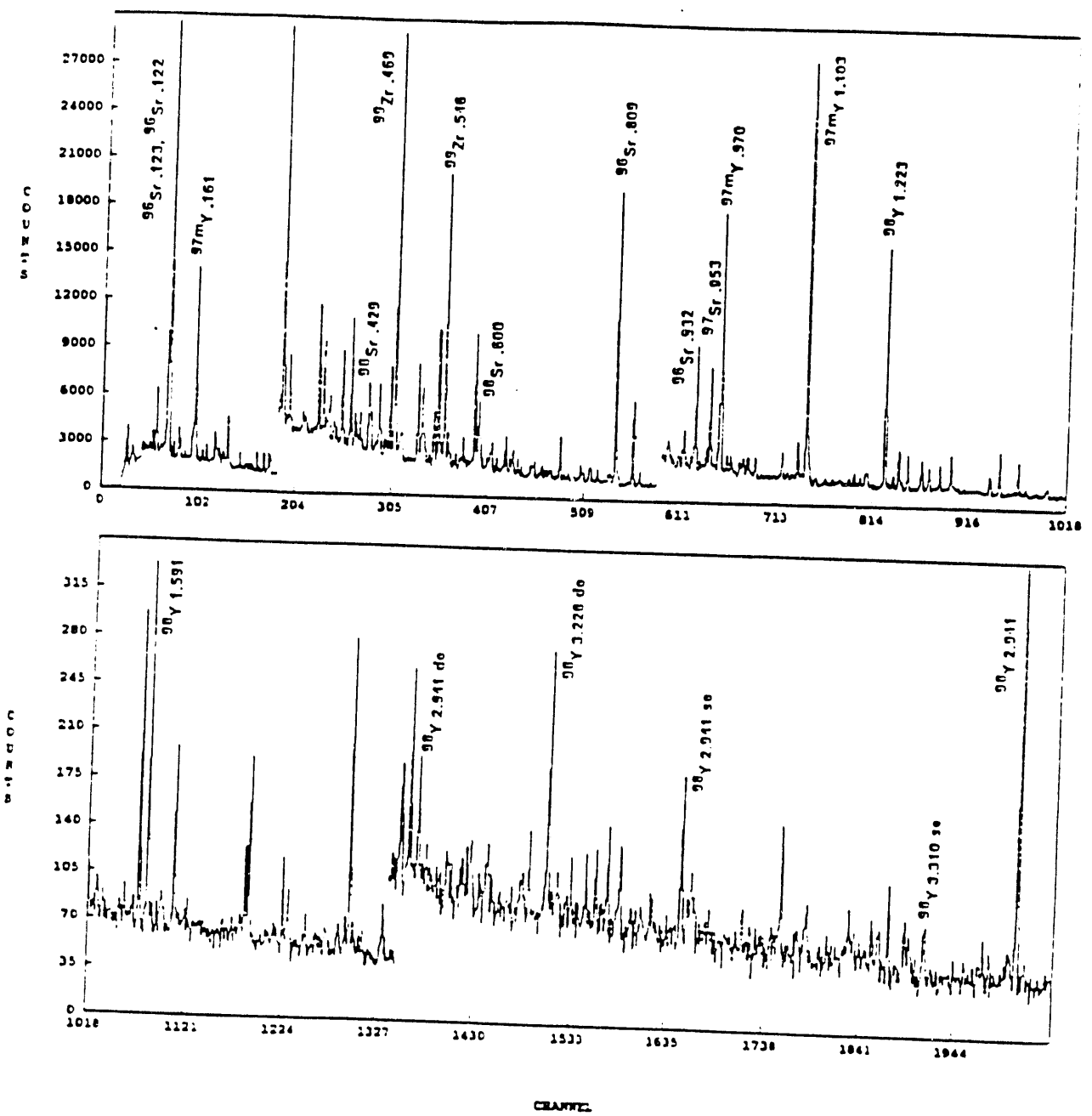

Fig. 15. *$^{235}U(n_{th},ff)$ gamma-ray spectrum with HPGe in the delay time interval 0.58 to 0.90 s. This spectrum covers gamma energies in 0 - 3 MeV range. Selective lines have been identified.*

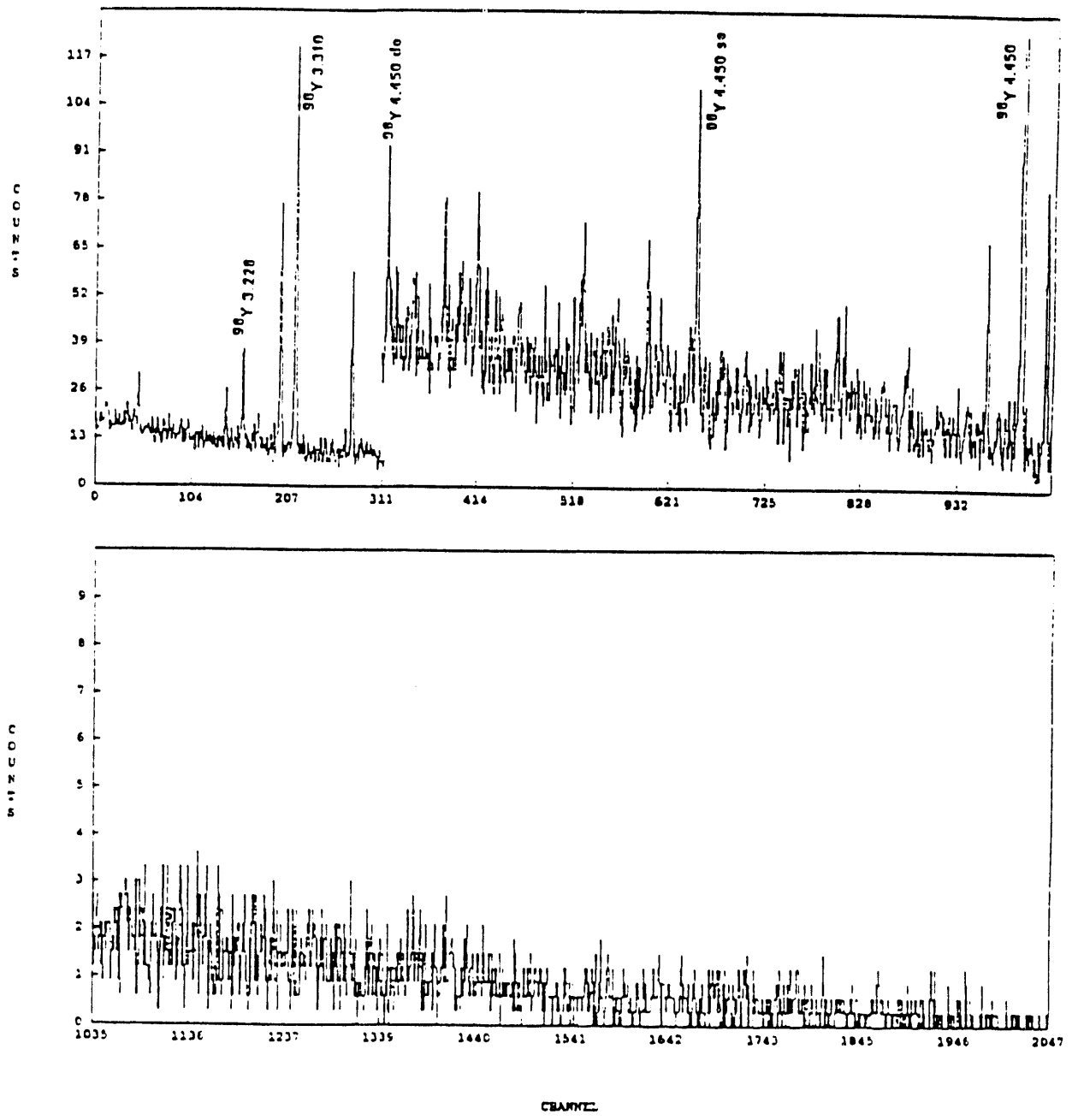

Fig. 16. The Fig. 15 spectrum plotted in the 3 - 6 MeV energy range.

Table II. Gamma ray lines extracted from the Fig.15-16 spectrum at 0.58 to 0.90s.

E (MeV)	Peak Area	E (MeV)	Peak Area	E (MeV)	Peak Area	E (MeV)	Peak Area	E (MeV)	Peak Area	E (MeV)	Peak Area
0.0584	6273	0.3560	312	0.7104	298	1.2284	62	1.9185	44	2.2503	30
0.0670	3286	0.3596	2808	0.7135	90	1.2351	129	1.9248	61	2.2848	177
0.0741	266	0.3634	622	0.7240	994	1.2442	396	1.9569	114	2.3086	287
0.0765	295	0.3680	1224	0.7298	180	1.2478	144	1.9826	110	2.3686	17
0.0817	1843	0.3752	536	0.7364	258	1.2578	322	1.9958	151	2.3875	19
0.0856	1282	0.3792	234	0.7462	112	1.2794	385	2.0094	101	2.3987	124
0.0926	1072	0.3876	2132	0.7558	402	1.2908	267	2.0553	55	2.4143	24
0.0973	1959	0.4005	2992	0.7597	262	1.3088	250	2.0798	48	2.4557	32
0.1028	6630	0.4069	686	0.7706	551	1.3215	59	2.0864	33	2.5457	30
0.1104	1167	0.4102	479	0.7822	343	1.3265	397	2.0932	85	2.5713	22
0.1147	1550	0.4147	963	0.7937	113	1.3316	80	2.1203	68	2.5966	33
0.1191	15699	0.4181	298	0.8010	336	1.3373	47	2.1727	55	2.6615	18
0.1186	9344	0.4289	1512	0.8094	7066	1.3646	57	2.1838	74	2.7582	12
0.1215	45513	0.4325	1027	0.8310	154	1.3847	241	2.2106	204	2.7632	23
0.1257	891	0.4401	406	0.8367	2302	1.3997	421	2.2253	49	2.8155	23
0.1301	1182	0.4447	1560	0.8471	396	1.4215	60	2.2452	45	2.8644	23
0.1377	3119	0.4561	492	0.8643	123	1.4275	285	2.2710	65	2.8852	20
0.1403	1910	0.4616	1974	0.8749	125	1.4389	92	2.2870	64	2.9285	15
0.1465	657	0.4690	9164	0.8782	155	1.4552	51	2.3051	82	2.9390	51
0.1513	311	0.4738	398	0.8841	107	1.4686	79	2.3248	92	2.9777	13
0.1610	22125	0.4796	21092	0.8912	315	1.4716	118	2.3422	35	4.0143	15
0.1725	1211	0.5039	1799	0.8952	105	1.4924	49	2.3576	35	4.1624	21
0.1792	2293	0.5109	2745	0.9069	135	1.5016	89	2.3749	41	4.1745	13
0.1872	797	0.5215	167	0.9145	346	1.5154	203	2.4203	141	4.2730	12
0.1925	4852	0.5293	1845	0.9251	92	1.5239	56	2.4301	47	4.3653	13
0.1988	2207	0.5359	4554	0.9314	1176	1.5484	47	2.4351	61	4.3964	29
0.2048	2210	0.5460	6779	0.9382	62	1.5562	77	2.4402	55	4.4155	11
0.2127	7350	0.5513	1085	0.9490	246	1.5678	64	2.4633	34	4.4500	183
0.2185	280	0.5547	422	0.9535	915	1.5772	454	2.5143	38	4.4897	47
0.2323	1402	0.5600	130	0.9693	2669	1.5904	514	2.5733	112	4.5504	9
0.2374	798	0.5639	255	0.9801	144	1.5970	58	2.6014	36		
0.2425	1096	0.5705	234	0.9864	187	1.6055	43	2.6146	60		
0.2472	895	0.5754	670	0.9994	98	1.6124	82	2.6793	41		
0.2514	892	0.5785	336	1.0046	188	1.6165	46	2.6883	36		
0.2588	1712	0.5835	222	1.0112	256	1.6326	304	2.6974	27		
0.2629	438	0.5895	241	1.0227	242	1.6538	55	2.7168	51		
0.2688	1768	0.5940	3384	1.0639	287	1.7227	38	2.7273	53		
0.2761	1522	0.6007	2463	1.0722	98	1.7361	85	2.7425	64		
0.2791	2555	0.6136	377	1.0895	380	1.7440	191	2.7681	62		
0.2847	358	0.6203	723	1.0956	122	1.7500	305	2.7747	49		
0.2918	859	0.6276	319	1.1030	4685	1.7864	49	2.8825	26		
0.2961	8583	0.6405	1014	1.1173	97	1.7904	52	2.8897	41		
0.3030	255	0.6472	307	1.1305	56	1.8011	133	2.8990	25		
0.3068	1654	0.6517	824	1.1419	71	1.8100	157	2.9281	28		
0.3103	256	0.6605	432	1.1485	56	1.8377	80	2.9307	31		
0.3257	186	0.6661	165	1.1531	79	1.8537	45	2.9412	369		
0.3285	517	0.6836	384	1.1670	85	1.8677	69	2.9531	30		
0.3325	555	0.6936	155	1.1756	120	1.8869	77	3.0626	39		
0.3408	124	0.6971	322	1.1848	97	1.8969	65	3.0630	43		
0.3459	263	0.7028	224	1.1945	281	1.9042	480	3.2010	54		
0.3520	2938	0.7067	223	1.2827	2135	1.9102	79	3.2277	79		

We have made preliminary beta count rate measurements over the delay time range of 0.75 to 40,000 seconds so as to compare to the data set of Dickens et al.[10] which extends between 2.7 and 12,000 seconds. Our results (activity x delay time, versus delay time) are compared to their ORNL data in Fig. 17. Both data sets display essentially the same character and agree well for most of the range of overlap except at short times, below 10 s, where our values appear somewhat higher. Possible explanations for this discrepancy, which will be further studied, are higher background near the helium jet spray point and effects of a low-energy beta cutoff in our data. In the Oak Ridge data, count rate effects, self absorption in the foils and rabbit walls, fission contributions from foils in the ambient neutron background and uncertainty in the delay-time values, particularly at short times, are perhaps significant factors contributing to this discrepancy.

The ORNL data include a correction for a loss of noble gases from their samples, e.g., an 11 % correction at 12,000 s. Noble gases are efficiently transferred in the helium jet but do not stick to the transfer tape so we too must correct our beta activity with an ENDF calculated component which equals 4% at 0.75 s and 19% at 40,000s. But we are able to collect the noble gases and their progeny using activated charcoal chilled to liquid nitrogen temperatures or simply a gas collector. Their activity can thus be measured with our system as demonstrated in Fig. 18 which shows a beta-coincidence Ge(Li) spectrum obtained from noble gases and their progeny. With some developmental work, it should be possible to measure these noble gas activities as a function of delay time and add their small contribution to the activity measured on the tape, rather than calculate this component.

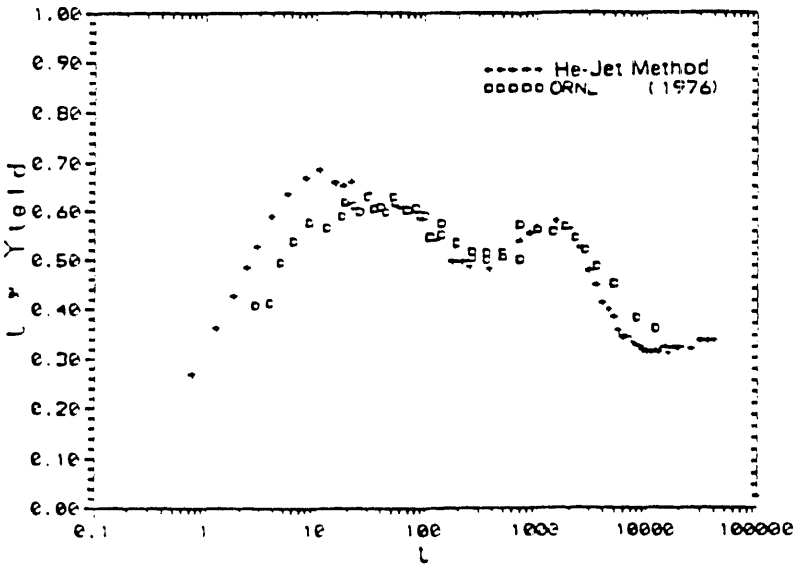

Fig. 17. Beta count rate comparison between our measurements and that of the ORNL group [Ref. 10] from the thermal fission of ^{236}U. The ORNL data consists of three sets normalized here to one another in regions of overlap. Both data sets include corrections for lost noble gas activities.

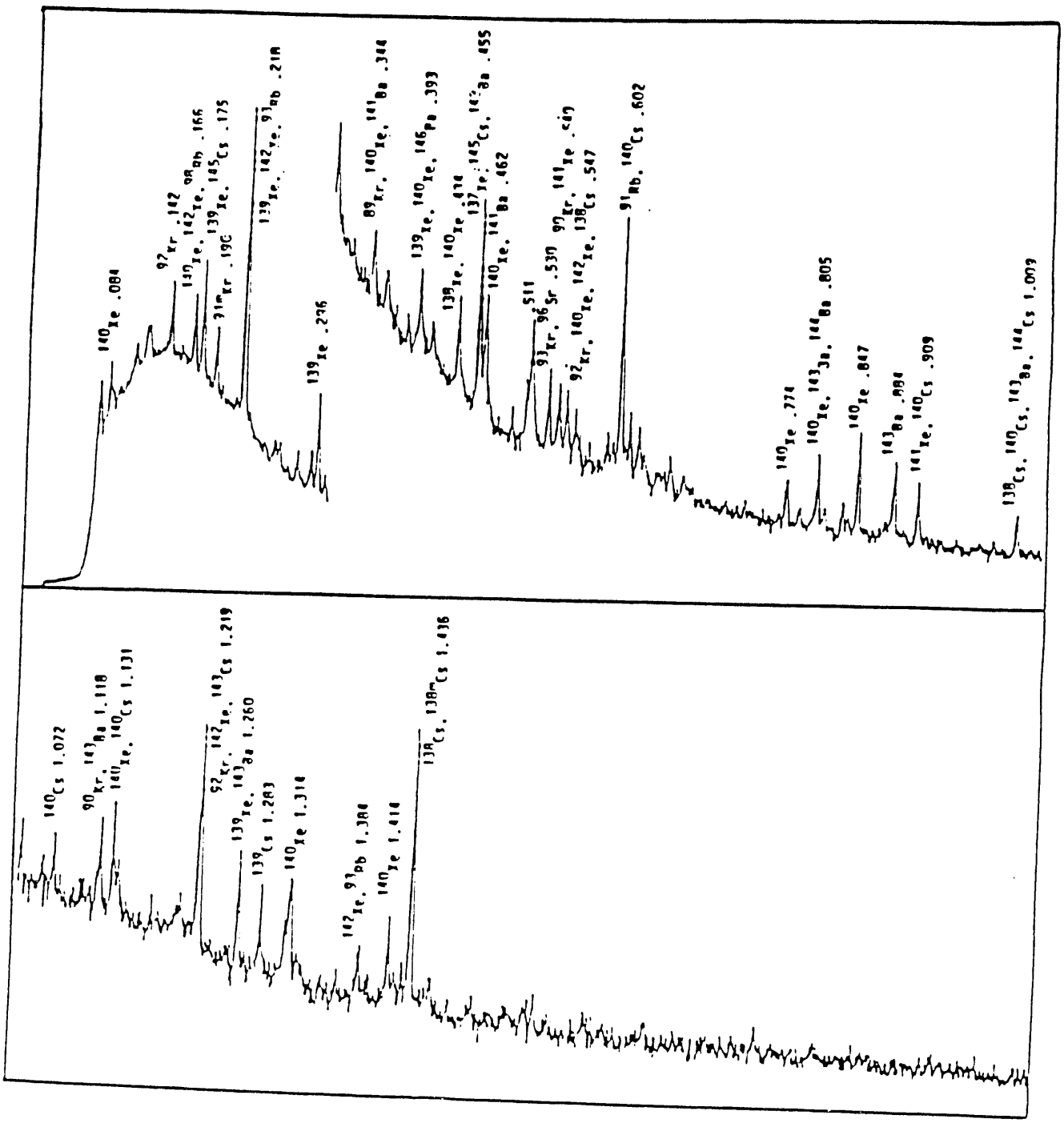

Fig. 18. *Gamma-ray spectrum measured with the helium jet displaying only transferred noble gas activities and their radioactive daughters.*

I. SPECTRUM ANALYSIS

Both the beta and gamma-ray energy spectra resulting from decay heat studies are continuous spectra that must be corrected for the response functions of their spectrometers to obtain the "true" energy distributions of the fission-product betas and gammas. To do so, each measured spectrum can be expressed as a superposition of response functions. The most suitable energy spacing for the response functions is about one half the width of the full-energy peak. As a result about 100 response functions are needed to represent the gamma-ray energy distribution and a somewhat smaller number for the beta energy spectrum. Since it's feasible to measure only 10-20 gamma response functions, we have developed interpolation programs for constructing response functions at any intermediate energy desired. The interpolation scheme has been completed for the beta responses and a similar, but more complex, procedure is being developed for the gamma-ray responses. The generated response functions are used as input files for FERDO, the spectral analysis program developed by Burrus[7] et al. for decomposition of continuous spectra. Development of the response-function interpolation method and the adaptation of the FERDO program for use on our computer system is the MS thesis project of Hung Nguyen.

The high-resolution gamma-ray spectra obtained with the HPGe detector are most useful in observing individual gamma-ray lines from the stronger fission-product contributors. In these spectra the weaker transistions merge with the Compton continuum and are thus treated as part of the background. This background subtraction is performed using an interactive graphics computer program, NDAA (developed by Dr. Marcel Villani). A subroutine of this program is used to fit background-subtracted peaks as a superposition of Gaussian peaks. The widths of the Gaussians are held fixed as determined by the energy-dependent peak-width calibration function. The number of peaks is specified by the user, and an initial guess of their positions is made. The program then optimizes the peak areas and peak positions using a non-linear least-squares fitting procedure. Fig. 19 shows a region of a gamma-ray spectrum following the fission of ^{235}U and the Gaussian fits obtained with the NDAA program.

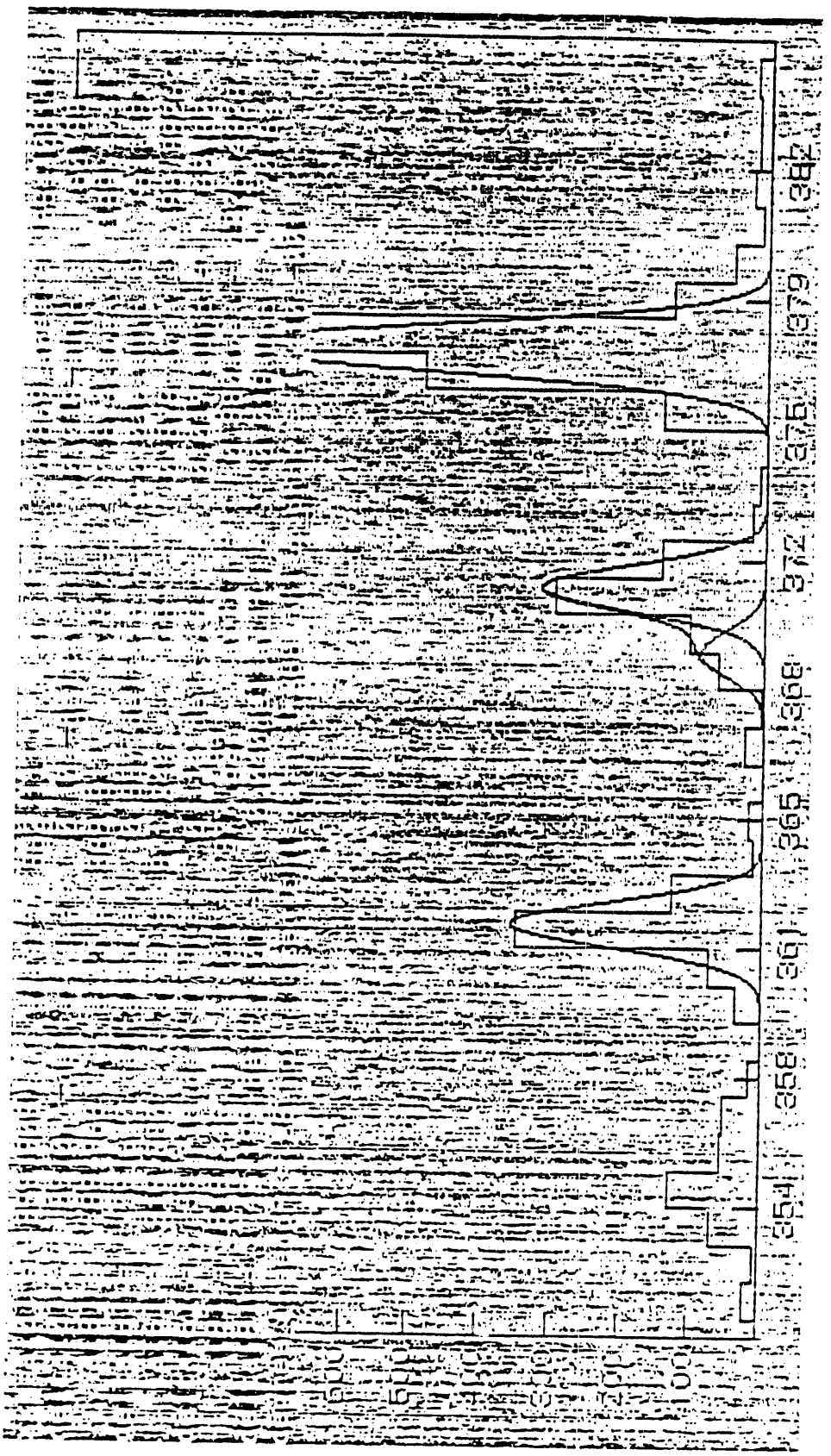

Fig. 19. Screen dump of the spectrum analysis program NDAA showing Gaussian fits.

J. HELIUM JET FISSION FRAGMENT TRANSFER EFFICIENCY STUDY

Prior to embarking on this decay heat study, we had established that the helium jet system transferred essentially the full distribution of fission fragments with a high degree of uniformity with only a few possible exceptions (e.g. the noble gases). This section presents improved transfer efficiency measurements comparing fission fragment transfer with a rabbit shuttle to that of the helium jet. X-rays are used as the signature for the transferred fission fragments. The relative transfer efficiency, therefore, is deduced from the ratio of the normalized x-ray intensities. To extract these intensities in the most precise and consistent manner, the background is subtracted using a filtering method. The resulting filtered spectra are least squares fitted with filtered model functions for each element. These model functions are generated using the known energies, relative intensities and detector energy resolution for the x-rays emitted by each element. Details follow:

The fission chamber of the helium jet was designed through its small size (and short capillary) to give both rapid and uniform transfer. The hemispherical 1.7-cm radius chamber is lined with thick ^{235}U foils. The escape probability is greater for the lighter, more energetic fission fragment as shown in Fig.20. But with the chamber at 4 atm. helium, one calculates[12] that these lighter fragments preferentially reimbed in the chamber walls and compensate for their excess escape probability. This leads to the nearly uniform stopping probability in the helium gas for all fission fragments as shown in Fig.20. The rabbit (a foam plastic cylinder) is shuttled between the neutron irradiated thick ^{235}U foil encompassing the rabbit and the x-ray detector (Fig.21). The exit of the helium-jet has a thin foam plastic "catcher" viewed by the Ge x-ray detector (Fig.22). The rabbit is shuttled back and fourth every 5 seconds giving it a delay time sensitivity that is a series of triangles extending out to the full length of the experimental run. The main improvement in this present transfer efficiency measurement was that we carefully matched the helium jet's time sensitivity to that of the rabbit shuttle by chopping the proton beam (on/off) and gating the MCA (off/on) to mimic the rabbit's 5-s irradiation and 5-s counting cycle in the accumulation of x-ray spectra.

Fig. 20. Fission fragment stopping probability in the helium of the fission chamber.

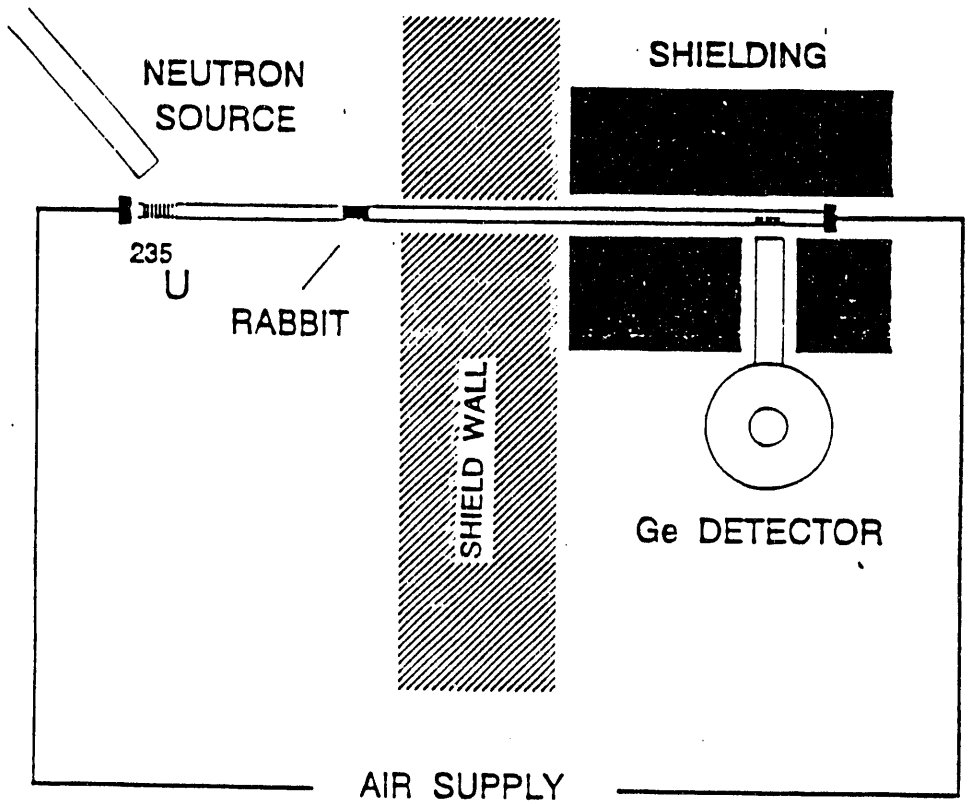

Fig. 21. Diagram of rabbit shuttle system uses in transfer efficiency measurements.

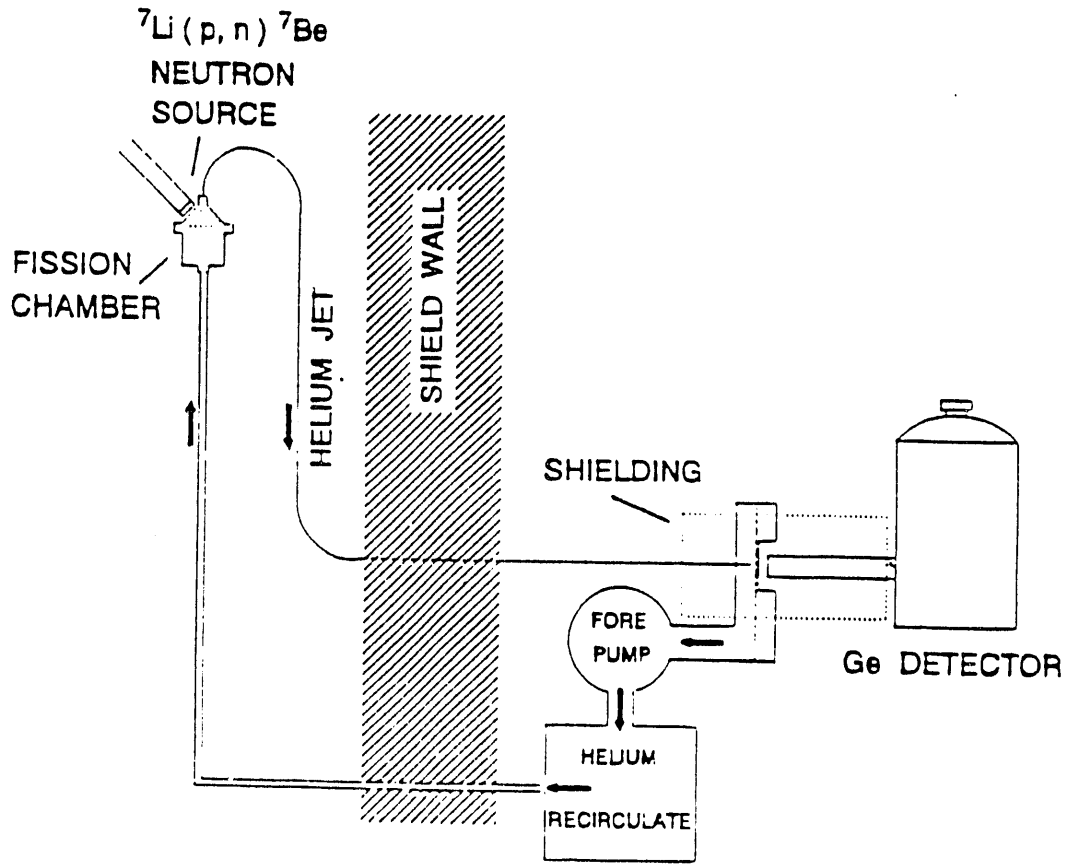

Fig. 22. Diagram of the helium-jet system used in the transfer efficiency study.

A visual comparison in Fig.23 made by superimposing x-ray spectra from the two systems demonstrates the high degree of uniformity. Of course, in the case of the rabbit shuttle, one expects the x-ray intensities for the lighter ("2/5 mass") group to exceed the heavier ("3/5 mass") group according to the thick foil escape probability in Fig.20 and upon inspection this appears to be the case.

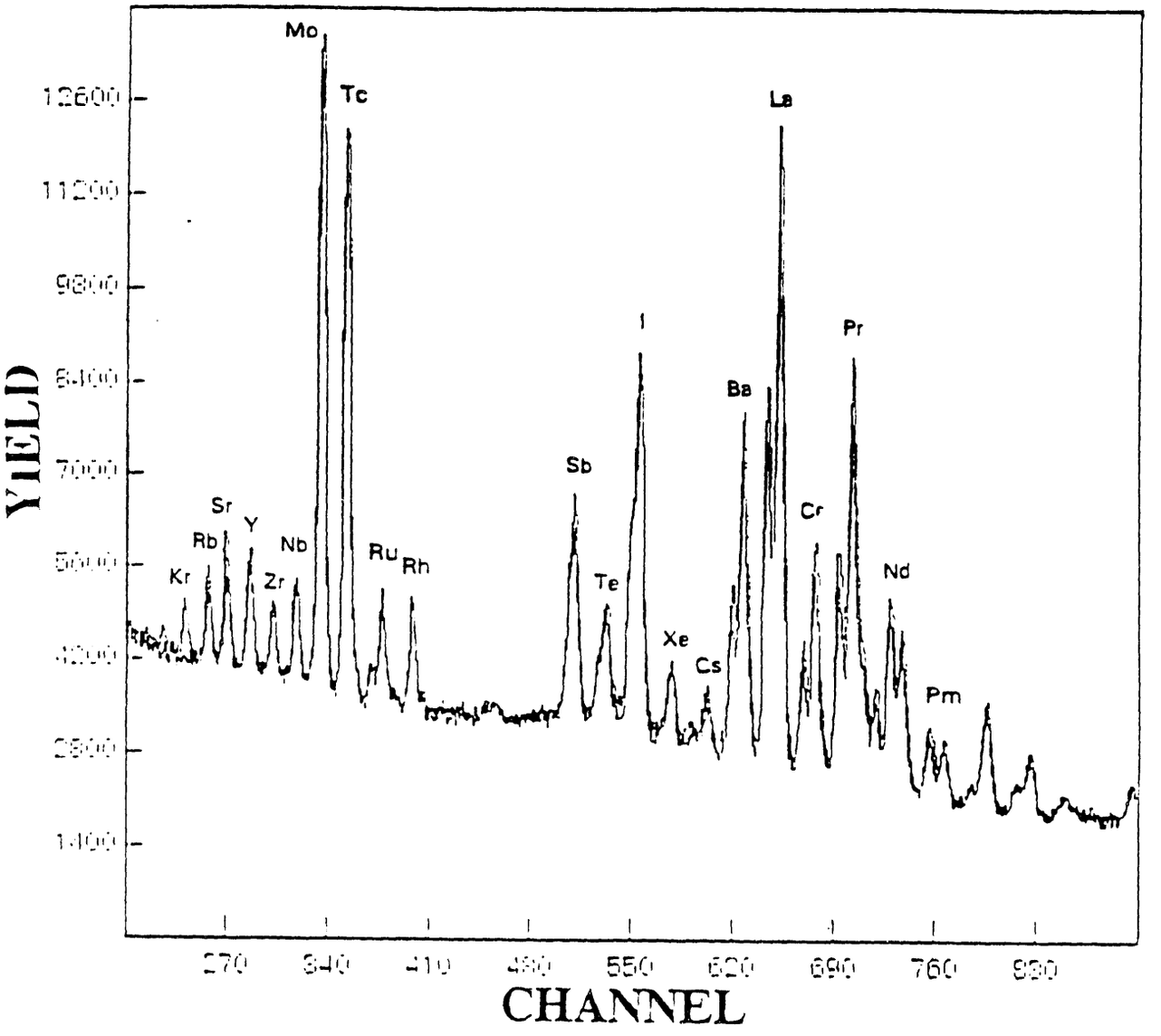

Fig. 23. Superimposed x-ray spectra from fission fragments transferred with the helium-jet and with the rabbit-shuttle system.

To extract x-ray peak intensities associated with a single element, two problems had to be addressed:

1) The overlapping peaks often hide the background, therefore, background subtraction could become somewhat subjective.
2) Although the resolution of the x-ray detector readily resolves the K_α lines of neighboring elements, the K_β lines from the Z-1 neighbor falls beneath the K_α.

A good solution to the background subtraction problem was to subject the spectra to an appropriately chosen filter which passes the peaks and rejects the background. This yields a background-free transform of the spectrum

$$y_i' = \sum_{j=-n}^{n} h_j y_{i+j}$$

The Gaussian weight function in Fig.24 is an appropriate filter to pass the x-ray peaks. When this filter is applied to a Gaussian "peak" in Fig.25, the transform basically retains the peak's character (e.g. its resolution). The second problem is addressed by using known information about the x-rays for each element, namely the energies and relative intensities of the $K_{\alpha 1}$, $K_{\alpha 2}$, $K_{\beta 1}$ and $K_{\beta 2}$ and the detector's energy resolution to form model spectra for each element represented in the spectrum. These models normalized to 10^4 counts are then sent through the same digital filter giving their transforms

$$m_i' = \sum_{j=-n}^{n} h_j Y_{i+j}$$

The relative intensities are extracted for each spectrum by performing a least squares fit of the filtered model spectra to the filtered measured spectrum

$$\chi^2 = \sum_{i=1}^{N} \left[\frac{\left(y_i' - \sum_{k=1}^{M} \sum_{i=1}^{N} a_k m_{ijk}' \right)^2}{\sum_{j=-n}^{n} h_j^2 y_{i+j}} \right]$$

where the a_k are the relative x-ray yields.

A representative least squares fitting of a filtered spectrum is presented in Fig.26 demonstrating how well the procedure works. Prior to forming ratios of the x-ray yields the rabbit data are divided by the escape probability to correct for that assymetry. Then ratios are calculated and normalized using the sums of the a_k values for each spectrum. This gives the helium-jet/rabbit intensity ratios presented in Fig. 27. It should be noted that the fission chamber design does properly correct for the light/heavy fission fragment escape probability. Nearly all masses appear to be transferred with equal probability. The loss of the Rb and Cs x-rays are interpreted as the loss of the noble gases, krypton and xenon, from the catcher. Such losses will be corrected by separate measurements of these missing components. This study is the M.S. thesis of Paul Bennett.

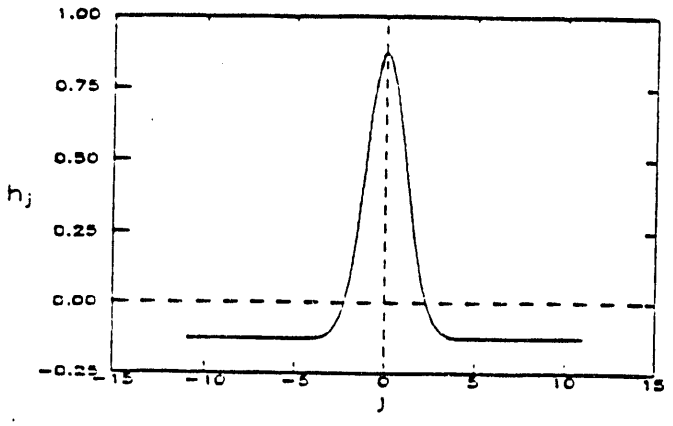

Fig. 24. Gaussian weight function used to remove background ($u = 1.6$, $v = 11$).

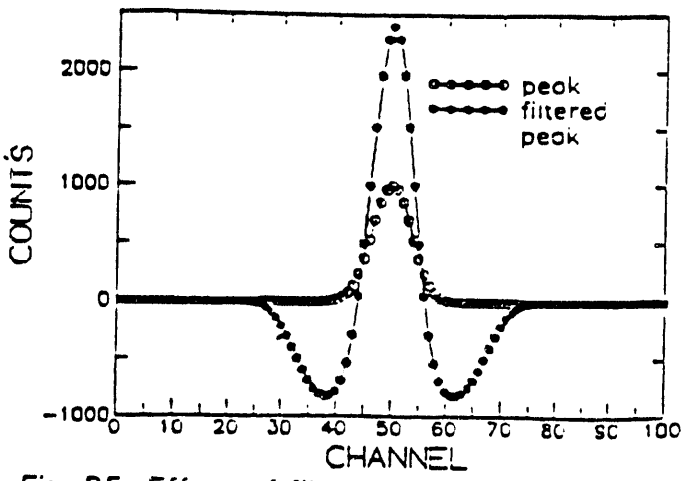

Fig. 25. Effect of filter applied to a Gaussian distribution.

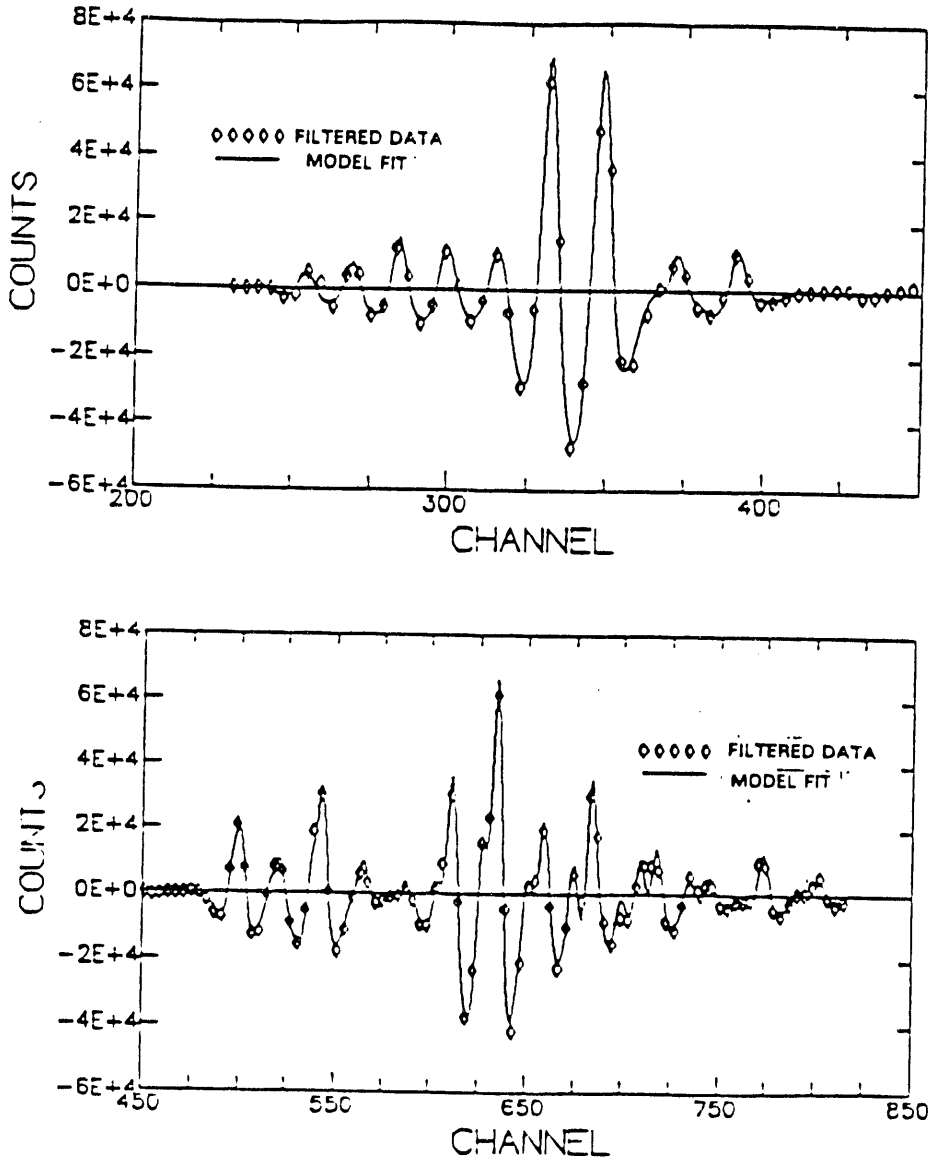

Fig. 26. Comparison of filtered x-ray data and model fit in the "2/5 mass region" (above) and "3/5 mass region" (below).

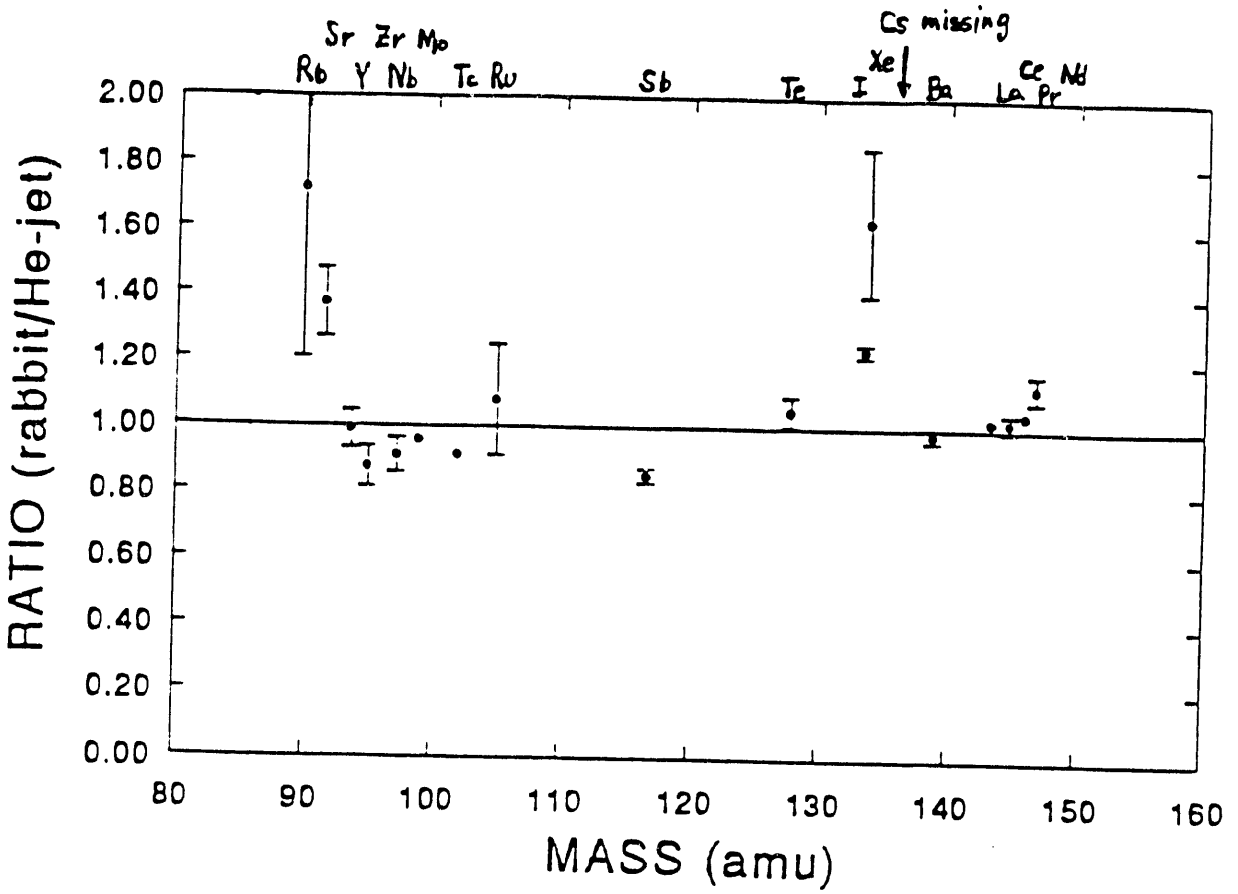

Fig. 27. *Ratio of x-ray intensities from fission fragment transfer with rabbit-shuttle and helium-jet systems. The ratio includes a correction for the escape probability from a thick ^{236}U foil.*

K. COMPARISON OF INDIVIDUAL GAMMA LINE INTENSITIES TO ENDF/B-VI

Prior to our recent HPGe measurements, a number of high resolution gamma ray spectra were obtained using a Ge(Li) detector and these have been analyzed to determine the time dependence of several prominant gamma lines in the interval below eight seconds. The time evolution of individual lines may be complex and not necessarily follow simple exponential decay, since fission products can be formed directly from fission or as a product in a beta-decay chain. Measured time dependences of individual lines can be compared with predictions based on summation calculations using data from ENDF/B-VI. These calculations are carried out with the LANL code CINDER and are facilitated by the collaborative effort between our group and Dr. T. England at LANL.

Some representative time dependences are shown in Figs.28 and 29, in which the relative positions of each gamma line in the vertical Log Yield axis are unnormalized. Lines drawn through data points for the individual gamma lines for each nuclide correspond to an average least squares fit for all gamma lines measured for the given nuclide, assuming simple exponential decay. The corresponding halflife is shown in the insert box. Also shown for each nuclide are the time evolutions predicted by CINDER. The lines drawn through the CINDER points are to guide the eye and do not represent CINDER output.

The time evolutions of the gamma-ray yields from the beta decay of ^{98}Zr and ^{96}Sr are seen to agree very well with CINDER. Slightly less satisfactory agreement is had for ^{97m}Y although the internal consistency in the measurements for the three identified gamma lines is extremely satisfactory. Four gamma lines resulting from ^{96}Sr beta decay are identified in the spectra based on their energies, and their time dependence corresponds to a halflife of 3.58s. This is markedly different from the value of 0.65s in the nuclear data file and represents the most significant discrepancy observed so far between our measurements and the data file. Time dependences for five lines originating from ^{96}Y and ^{96m}Y beta decays are shown in the final figure. Four of these lines exhibit the same time dependence and according to the CINDER calculations are in apparent agreement with the ground state decay of ^{96}Y. The fifth line agrees best with the CINDER calculation for the metastable state decay. However, the halflives assumed in the CINDER (ENDF) calculations for the ground state and metastable state decays are reversed in the nuclear data sheets and therefore identification of the state of origin for these lines is ambiguous.

At longer delay times, a buildup of activity from the beta chain contribution becomes evident. As examples of this buildup, Fig. 30 presents CINDER (ENDF/B-VI) comparisons for the ^{99}Nb, ^{143}Ba and ^{146}La cases. The HPGe spectrometer with its better resolution and background suppression will provide far more lines to study. This study forms parts of the Ph.D. theses of Joann Campbell and Sameer Tipnis.

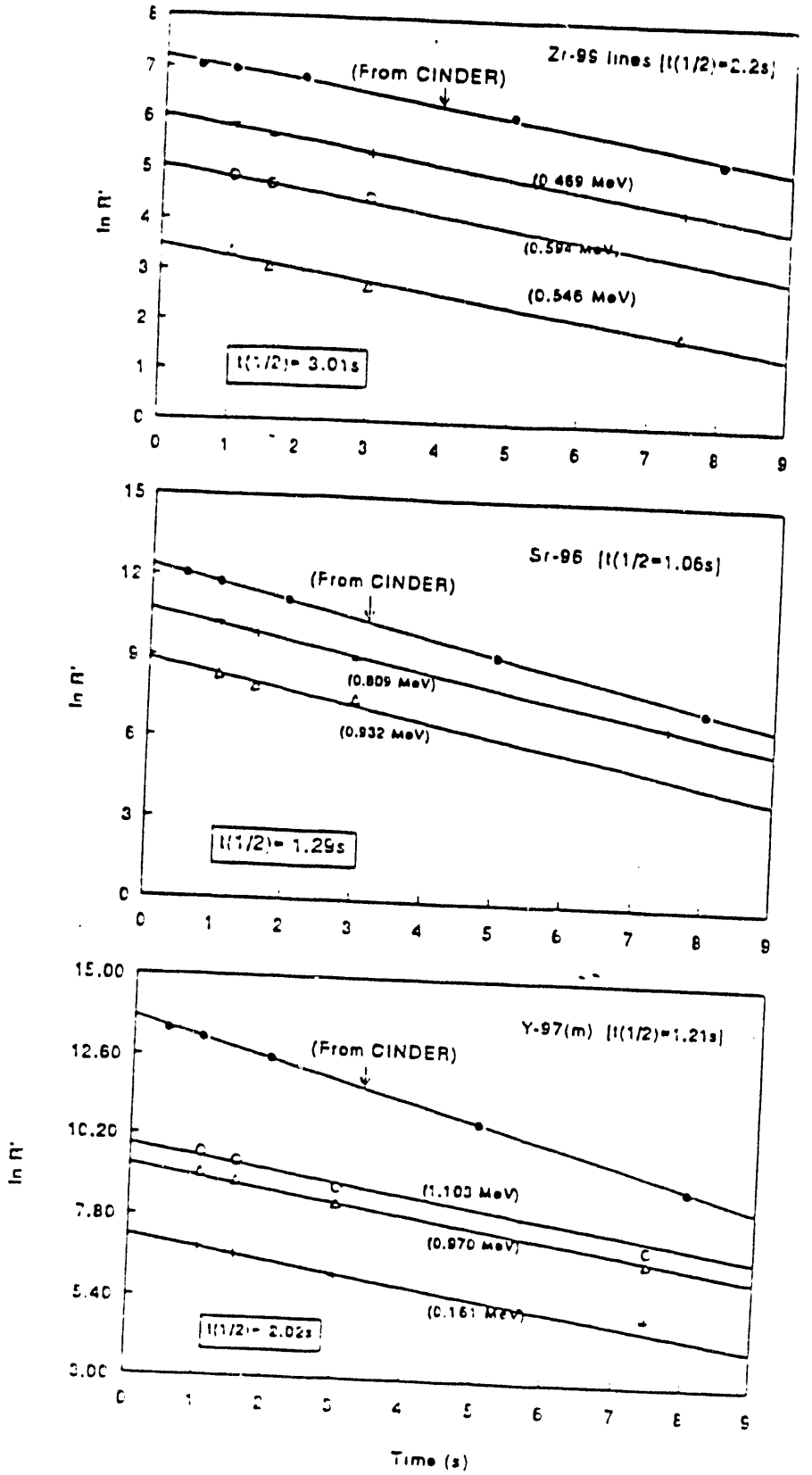

Fig. 28. *Comparison of our normalized gamma line intensities to CINDER (ENDF/B-VI) predictions for ^{99}Zr, ^{99}Sr and ^{97m}Y.*

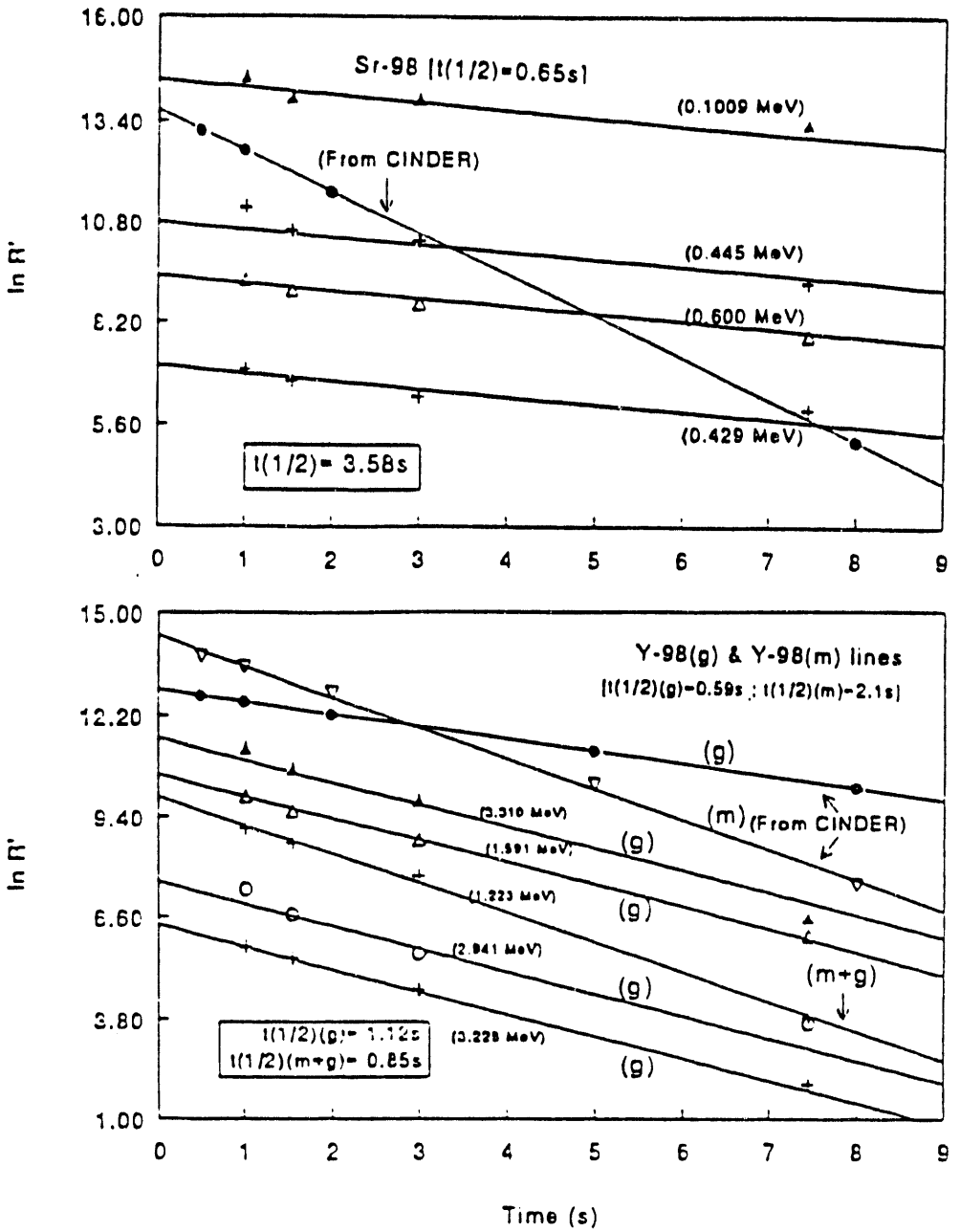

Fig. 29. Comparison of our normalized gamma line intensities to CINDER (ENDF/B-VI) predictions for ^{96}Sr and ^{96}Y, ^{96m}Y.

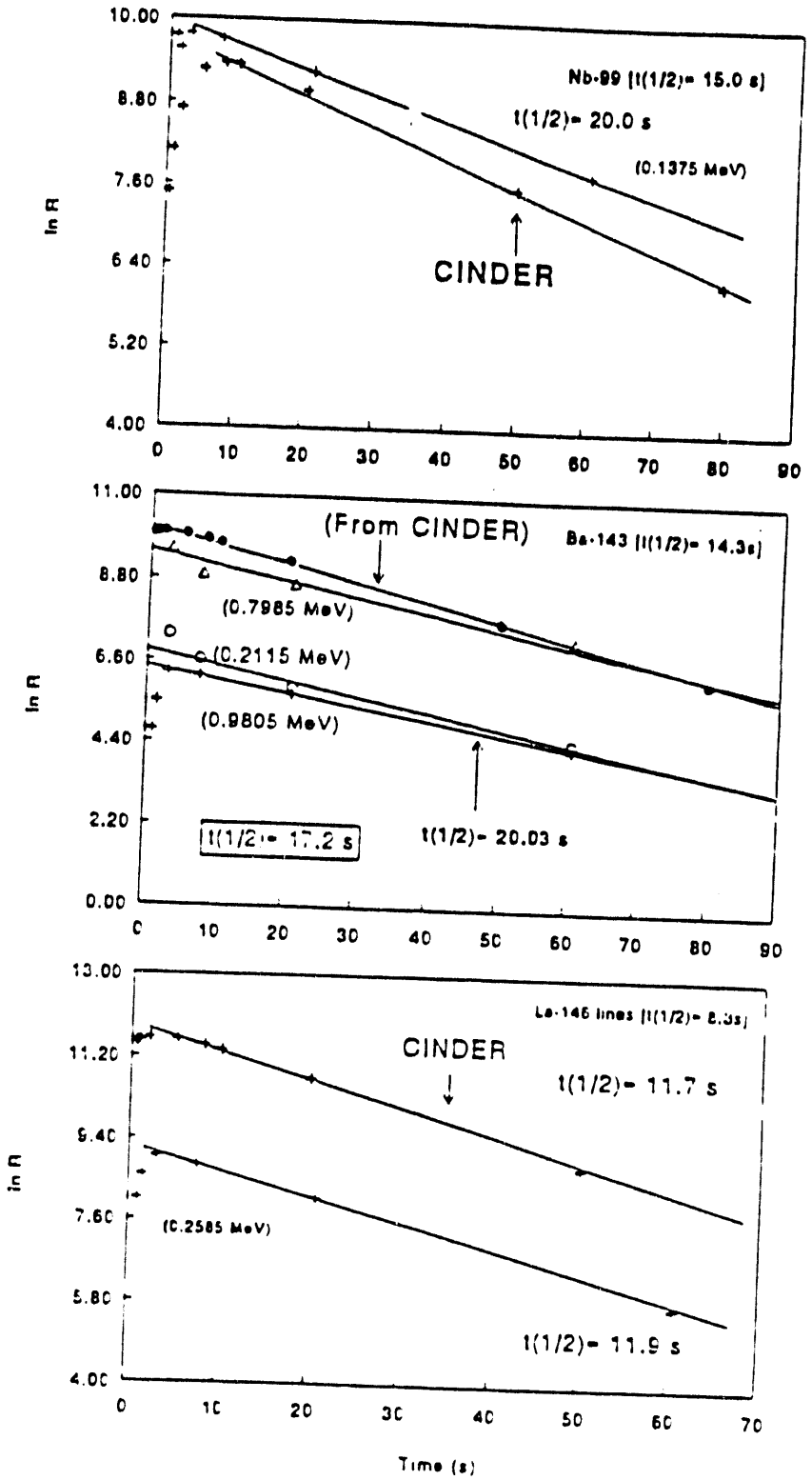

Fig. 30. *Comparison of our normalized gamma line intensities to CINDER (ENDF/B-VI) predictions for ^{99}Nb, ^{143}Ba and ^{146}La. At these longer delay times buildup becomes evident.*

PUBLICATIONS

Published Abstracts

1. D.J. Pullen, J.M. Campbell, G.P. Couchell, H.V. Nguyen, W.A. Schier, S.V. Tipnis and M. Villani, "Use of a High Purity Germanium Detector in Aggregate Fission-Product Decay Heat Studies", Bull. Am. Phys. Soc. **37**, 1276 (1992).

2. G.P. Couchell, J.M. Campbell, H.V. Nguyen, D.J. Pullen, W.A. Schier, S.V. Tipnis, M.F. Villani, "A NaI(Tl) Gamma-Ray Spectrometer for Aggregate Fission Product Gamma Decay Heat Study". Bull. Am. Phys. Soc. **37**, 1292 (1992).

3. W.A. Schier, J.M. Campbell, G.P. Couchell. H.V. Nguyen, D.J. Pullen, S.V. Tipnis and M.F. Villani, "Beta Spectrometer Design and Testing", Bull. Am. Phys. Soc. **37**, 1293 (1992).

4. P.R. Bennett, J.M. Campbell, G.P. Couchell, H.V. Nguyen, D.J. Pullen, W.A. Schier, S.V. Tipnis, M.F. Villani, "Helium Jet Fission Fragment Transfer Efficiency", Bull. Am. Phys. Soc. **37**, 1293 (1992).

5. M.F. Villani, J.M. Campbell, G.P. Couchell, D.J. Pullen and W.A. Schier, "Six-Group Decomposition of ^{238}U Delayed Neutron Composite Energy Spectra", Bull. Am. Phys. Soc. **37**, 1300 (1992).

6. J.M. Campbell, G.P. Couchell, T.R. England, H.V. Nguyen, D.J. Pullen, W.A. Schier, S.V. Tipnis and M.F. Villani, "Comparison of Selective Gamma-Ray Yields following Thermal Fission of ^{235}U with the ENDF/B-VI Decay Data", Bull. Am. Phys. Soc. **37**, 1300 (1992).

Abstracts Submitted to New England Section of Am. Phys. Soc. Meeting, April 2-3, 1993

7. "High-Resolution Gamma-Ray Study of Aggregate ^{235}U Fission Products", J.M. Campbell, G.P. Couchell, S. Li, H.V. Nguyen, D.J. Pullen, W.A. Schier and S.V. Tipnis

8. "Study of Gamma-Ray Decay Heat from Aggregate ^{235}U Fission Products", G.P. Couchell, J.M. Campbell, S. Li, H.V. Nguyen, D.J. Pullen, W.A. Schier and S.V. Tipnis

9. "Response Functions for Beta-Particle and Gamma-Ray Spectrometers", S. Li, J.M. Campbell, G.P. Couchell, H.V. Nguyen, D.J. Pullen, W.A. Schier and S.V. Tipnis

10. "Spectrum Analysis Programs for Decay Heat Studies of Aggregate Fission Products", H.V. Ngugen, J.M. Campbell, G.P. Couchell, S. Li, D.J. Pullen, W.A. Schier and S.V. Tipnis,

11. "Comparison of the Measured Time-Evolution of Individual Fission-Product Gamma-Ray Lines with ENDF/B-VI", S.V. Tipnis, J.M. Campbell, G.P. Couchell, T.R. England, S. Li, H.V. Nguyen, D.J. Pullen and W.A. Schier

12. "Study of Beta-Particle Decay Heat from Aggregate ^{235}U Fission Products", J.M. Campbell, W.A. Schier, G.P. Couchell, S. Li, H.V. Nguyen, D.J. Pullen and S.V. Tipnis

Journal Publications

1. M.F. Villani, G.P. Couchell, M.H. Haghighi, D.J. Pullen, W.A. Schier and Q. Sharfuddin, "Six-Group Decomposition of Composite Delayed Neutron Spectra from ^{235}U Fission", Nucl. Sci. Eng. 111, 422 (1992).

FACULTY REASEARCH ASSOCIATE

Dr. David Pullen

STUDENTS ASSOCIATED WITH THE PROJECT

Graduate Students

Paul Bennett (M.S.) *

Joann Campbell (Ph.D.)

Shengjie Li (Ph.D.)

Hung Nguyen (M.S.)

Edward Seabury (Ph.D.)

Sameer Tipnis (Ph.D.)

Marcel Villani (Ph.D.)

* Presently employed as staff scientist at Radiation Monitoring Devices, Inc., Watertown, MA 02172

Degrees Conferred on Students Associated with Project

Marcel Villani, Ph.D.(presently in a postdoctoral appointment at Nuclear Physics Lab of University of Kentucky)

RESEARCH TIME COMMITMENT OF PI'S AND FACULTY ASSOCIATE

During the past nine months, the principle investigators, Walter Schier and Gus Couchell, have each devoted two summer months to the project and more than a day/week during the fall and spring semesters. This commitment will continue during the remainder of the current term. The faculty associate, David Pullen, made a similar two-summer month commitment and one day/week during the semesters.

References

1. G. Rudstam and T. England, Test of Pre-ENDF/B-VI Decay Data and Fission Yields, LA-11909-MS (1990).

2. J. K. Dickens, "Fission Product Decay Heat for Thermal Reactors," Proc. Int. Conf. Nuclear Cross Sections for Technology, Knoxville, TN, Oct. 22 - 26, 1979, pp. 25-33 (1980).

3. W. A. Schier, G. P. Couchell, D. J. Pullen, N. M. Sampas, C. A. Ciarcia, M. H. Haghighi, Q. Sharfuddin and R. S. Tanczyn, Nucl. Instrum. Methods, Phys. Res., 227, 549 (1984).

4. R. S. Tanczyn, Q. Sharfuddin, W. A. Schier, D. J. Pullen, M. H. Haghighi, L. Fisteag and G. P. Couchell, Nucl. Sci. Eng. 94, 353 (1986).

5. G. Couchell, P. Bennett, E. Jacobs, D. Pullen, W. Schier, M. Villani, R. Tanczyn, M. Haghighi, Q. Sharfuddin, "Composite Delayed Neutron Energy Spectra of Fissionable Isotopes," 50 Years With Nuclear Fission, Vol. 1, pp. 449 - 456, ISBN 0-89448-144-4, Publ. by Amer. Nucl. Soc., La Grange Park, Illinois (1989).

6. C. W. Reich, "Review of Nuclear Data of Relevance for the Decay Heat Problem," Proc. Spec. Meeting Data for Decay Heat Predictions, Studsvik, Sweden, 7 - 10 September, 1987, pp. 107 - 118 (1987).

7. B.W. Rust, D.T. Ingersoll and W.R. Burrus, A User's Manual for the FERDO and FERD Unfolding Codes, ORNL/TM-8720 (1983).

8. K. Takahashi and M. Yameda, Prog. Theor. Phys. 41, 1470 (1969).

9. T. Yoshida and J. Katakura, Nucl. Sci. Eng. 93, 193 (1986).

10. J. Katakura and T. England, "Augmentation of ENDF/B Fission Product Gamma-Ray Spectra by Calculated Spectra," to be published by Los Alamos National Laboratory.

11. J. K. Dickens, T. A. Love, J. W. McConnell and R. W. Peelle, Nucl. Sci. Eng., 74, 106 (1980).

12. R. S. Tanczyn, G. P. Couchell and W. A. Schier, Computer Phys. Comm. 39

DATE
FILMED
6/7/93